Adaptive Control of Hydraulic Shift Actuation in an Automatic Transmission

by

Sarah Marie Thornton

B.S. Mechanical Engineering
University of California at Berkeley, 2011

Submitted to the Department of Mechanical Engineering
in partial fulfillment of the requirements for the degree of

Master of Science in Mechanical Engineering

at the

MASSACHUSETTS INSTITUTE OF TECHNOLOGY

June 2013

Author .....
Department of Mechanical Engineering
May 10, 2013

Certified by .....
Dr. Anuradha Annaswamy
Senior Research Scientist
Thesis Supervisor

Accepted by .....
David E. Hardt
Chairman, Department Committee on Graduate Students

Adaptive Control of Hydraulic Shift Actuation in an Automatic Transmission

by

Sarah Marie Thornton

Submitted to the Department of Mechanical Engineering
on May 10, 2013, in partial fulfillment of the
requirements for the degree of
Master of Science in Mechanical Engineering

Abstract

A low-order dynamic model of a clutch for hydraulic control in an automatic transmission is developed by separating dynamics of the shift into four regions based on clutch piston position. The first three regions of the shift are captured by a physics-based model and the fourth region is represented by a system identification model. These models are determined using nominal values and validated against nominal and off-nominal experimental data. The model provides two lumped flow parameters to be used for tuning to the desired hydraulic clutch system.

Using feedback information from the model and transmission mechanicals, a closed -loop adaptive controller is designed. The controller is structured to update at three different rates: every time instance, every shift, and every n-th number of shifts. Part of the controller is designed to operate in open-loop for the first two regions of the shift until feedback information is available. The open-loop controller adapts within the shift, thus allowing for corrections to the control design to be made in following shifts. The model tuning parameters as well as the main spring preload become the adaptive parameters, which are then adjusted so that the plant matches the model. The control design is validated against a high fidelity simulation model of the transmission hydraulics and mechanicals.

Thesis Supervisor: Dr. Anuradha Annaswamy
Title: Senior Research Scientist

Acknowledgments

Dr. Annaswamy, thank you for the opportunity to work with you on this project. Your guidance and expertise have taught me many new skills as a researcher.

To my colleagues at the Ford Motor Company:

Thank you Diana Yanakiev for your mentorship and knowledge throughout this project. It has been a real pleasure working alongside you, thus allowing me to gain confidence in my abilities as a researcher.

Thank you Greg Pietron for your major contribution in developing the model of the hydraulic clutch actuation. Also, thank you for always critizing my data visualizations, thus teaching me the importance of proper graphical communication. In addition, thank you for allowing me and Diana to continually bother you with our questions about the complicated behavior of the transmission.

Thank you James McCallum for your high fidelity transmission simulation model as well as for your quiet tolerance of our many meetings.

Lastly, thank you to Joseph Kucharski for your help in gathering vehicle data.

I would like to thank all my friends at MIT for the study groups and many positive memories. My time here would not have been the same without you all to share it with.

I would especially like to thank my husband, Joseph, for his sacrifice and patience while his wife travelled to the otherside of the country in pursuance of this experience. I would not have made it without your love and encouragement.

Finally, I would like to thank God for always being with me.

This work was supported by the Ford Motor Company. Additionally, I was partially supported by the National Science Foundation through a graduate fellowship.

Contents

List of Figures

THIS PAGE INTENTIONALLY LEFT BLANK

List of Tables

THIS PAGE INTENTIONALLY LEFT BLANK

Chapter 1

Introduction

1.1 Problem Motivation

When a person drives or rides in a vehicle equipped with an automatic transmission, they often notice when a "bad" shift occurs. With respect to all vehicle occupants, they are likely to perceive a "bad" shift when there is a torque disturbance to the driveline or an unexpected increase in engine speed. With respect to the driver and when they command the throttle input, a "bad" shift may be the result of a delay in the shift from their input or because the shift takes a long time to complete. In the case of synchronous shifting, these are a result of the on-coming (ONC) clutch and the off-going (OFG) clutch not coordinating correctly as seen in Fig. 1-1.

In a typical powertrain control strategy, there is no on-board sensing that provides feedback about the response of the clutches before the gearbox speed measurements start changing. For a synchronous power-on upshift, it means there is no feedback during the initial hydraulic actuation of the clutches and through the torque transfer phase. Only after the speed ratio change commences is the real-time controller in a position to issue its commands based on feedback information.

The dynamics of the hydraulic clutch actuation system is highly nonlinear with mostly unobservable conditions. Additionally, feedback information from direct measurements during shift is not available until the end of the shift during the inertia transfer phase when shaft speed signals arise. Since the shaft speed signals do not

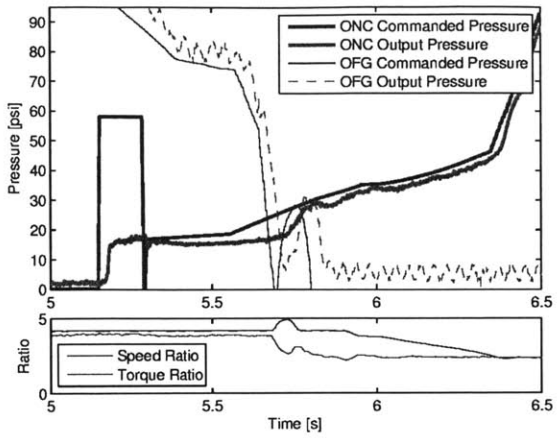

Figure 1-1: Example of undesired shift event depicted in the pressure domain achieved by purposely altering the open-loop pressure command of the ONC clutch as well as torque and speed ratio changes.

arise until the end of the shift, it is typically used after the completed shift, which is too late to improve the quality of that shift. As a result, the control strategy is conducted mostly in open-loop, excluding the inertia transfer phase. Because of a lack of robustness and consistency as well as poor disturbance rejection properties often attributed with open-loop control, current control strategies compound a learning algorithm with the open-loop controller in an attempt to update key parameters. However, this is achieved by purposely allowing "bad" shifts to occur in order to improve the next shift.

Since these open-loop control strategies have major drawbacks, assimilating additional closed-loop control methods for shift control would be advantageous. In order to incorporate such methods, measurements or estimates of the shaft torque are needed. The work done in [14] suggests that estimation of the shaft torque for shift control is achievable through the use of measurements of the output shaft speed and wheel speed in a sliding mode nonlinear observer. Information from the shaft torque can be used to calculate the clutch torque, which would be beneficial to employing adaptive algorithms to help the robustness and consistency of disturbance rejection of the open-loop control.

1.2 Literature Review

A model is needed to better understand the hydraulic clutch actuation prior to the availability of feedback signals in the powertrain. The powertrain modeling in [1] includes a relatively low order model of the engine, transmission mechanicals and drivetrain. However, this model does not include an adequate representation, perhaps intentionally, of the clutch hydraulic actuation since hydraulics can vary in implementation and would thus distract from their intent of maintaining generality of the model. Instead, they use a clutch pressure profile based on empirical data. For simulation purposes, it is also assumed in [1] that the relationship between clutch pressure and clutch torque capacity is linear during the shift, which is only true after the clutch hydraulic actuation transients. Similarly, the models in [10] and [9] also focused on maintaining generality, but validated the model via closed loop PID control of the inertia transfer phase.

The works done by [16], [17] and [2] are more closely related to our goal of modeling the hydraulic actuation of a clutch in an automatic transmission. In [16], system identification techniques are used to obtain a second order transfer function model of the actuation. However, it assumes the pre-load pressure of the clutch spring as well as the stroke pressure are known in order to switch between the different phases of the shift. Also, there is a loss of detail of the nonlinear dynamics of the shift in the first two phases, which is crucial to determine whether the pre-load and stroke pressures are correct. If Newtonian dynamics are used to derive the clutch model, it results in a high order model like that derived in [17]. Even though [17] uses an energy based model reduction method by [13], the resulting model order is still not desirable and also loses the details of determining the stroke pressure. If pressure measurements are available, then a linear, low order, discrete-time model such as that used by [2] would be a good method. However, these pressure measurements are not always available, and this thesis operates under the assumption that pressure measurements are not available in the hydraulic line of the transmission.

1.3 Outline of this Thesis

The remainder of this thesis is organized as follows: Chapter 2 details the low order hydraulic clutch actuation model. Shift dynamics are explained in section 2.2. Section 2.3 presents the system identification model and the control-oriented model is detailed in section 2.4. Section 2.5 presents the model validation using nominal and off-nominal conditions. Chapter 3 discusses the adaptive closed-loop control design and open-loop control design. Concluding remarks and future work are given in Chapter 4.

Chapter 2

Hydraulic Clutch Actuation Model

2.1 Introduction

When a person drives or rides in a vehicle equipped with an automatic transmission, they often notice when a "bad" shift occurs. With respect to all vehicle occupants, they are likely to perceive a "bad" shift when there is a torque disturbance to the driveline or an unexpected increase in engine speed. With respect to the driver and when they command the throttle input, a "bad" shift may be the result of a delay in the shift from their input or because the shift takes a long time to complete. In the case of synchronous shifting, these are a result of the on-coming (ONC) clutch and the off-going (OFG) clutch not coordinating correctly.

In a typical powertrain control strategy, there is no on-board sensing that provides feedback about the response of the clutches before the gearbox speed measurements start changing. For a synchronous power-on upshift, it means there is no feedback during the initial hydraulic actuation of the clutches and through the torque transfer phase. Only after the speed ratio change commences is the real-time controller in a position to issue its commands based on feedback information.

We propose a new model that combines physical equations and system identification techniques in order to capture details of the hydraulic clutch actuation in a low order form. To achieve representation of the specifics in the actuation, we partition the shift dynamics into four regions based on the clutch piston position. A

physics-based model characterizes the first three regions of the shift, thus capturing the dominant dynamics of the shift using one state, the clutch piston position. In the second and third regions, two lumped parameters are chosen to characterize the flow dynamics, whose values are determined using a combination of physical insight and tuning using experimental data from a rear-wheel drive passenger vehicle with a six-speed automatic transmission. Data from nominal conditions were used as training data and those from off-nominal conditions were used as testing data.

The resulting overall model is expected to feature a much better ability to determine stroke pressure and monitor the behavior of the clutch piston position. It is intended for use in alleviating the problem of open-loop control which may lead to "bad" shifts, especially at the beginning of the shift.

2.2 Shift Dynamics

An automatic transmission with a planetary gearbox has several friction elements (clutches) that alter the kinematic arrangement of the gearbox to provide different gear ratios. The hydraulic control system provides the actuation for the clutches to perform the desired torque and speed ratio changes for the commanded shift.

2.2.1 Power-on Upshift

In a power-on upshift, the torque ratio changes first, as both clutches transmit positive torque to the gearbox output. The speed ratio changes after the torque transfer is complete.

Torque transfer phase. During the torque phase the ONC clutch and the OFG clutch trade the transmission load. Once the hydraulic lines of the ONC clutch are pressurized, it gains torque capacity and establishes a power path with less resistence. As it is further applied, it carries more torque and this results in the OFG clutch being unloaded. It is essential to release the OFG clutch once its torque reaches zero, because keeping it beyond that would lead to it applying opposing effort, a.k.a. "tie-up". In contrast, if it is realeased too early, before the ONC clutch has enough

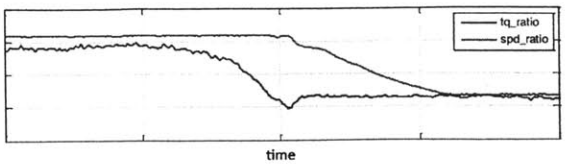

Figure 2-1: Example of smooth torque and speed ratio changes.

capacity to carry all the torque, a neutral-like condition will occur. Output shaft torque would drop further and engine speed would increase unnecessarily. The torque transfer phase is best visualized through the torque ratio change in Fig. 2-1.

Inertia transfer phase. When the torque transfer phase is complete, the inertia transfer phase begins. The ONC clutch carries the full transmission load and continues increasing torque capacity to control the desired speed ratio change. This causes the gear connected to both sides of the ONC clutch to synchronize in speed as the torque capacity increases until it can be engaged without disturbance. At that point, the ONC clutch will lock-up and the shift is complete. The inertia transfer phase is best visualized through the speed ratio change in Fig. 2-1.

2.2.2 Power-On Downshift

In a power-on downshift, the order of the transfer phases switch. The OFG clutch slips to change the speed ratio first, while the ONC clutch prepares to stroke for the torque transfer phase. Once the inertia transfer phase completes, the ONC clutch is ready to begin the torque transfer phase.

2.2.3 Hydraulic Clutch System

The torque and inertia transfer phases are a result of the actuation in the hydraulic clutch system, which is the focus of this thesis. A hydraulic clutch system uses a pump to feed the hydraulic fluid throughout the entire system. The pump supplies the line pressure, which controls the maximum amount of pressure available in the system at a given instance. The control input is the commanding pressure of a variable force solenoid. Once commanded, the hydraulic fluid flows through the regulator valve,

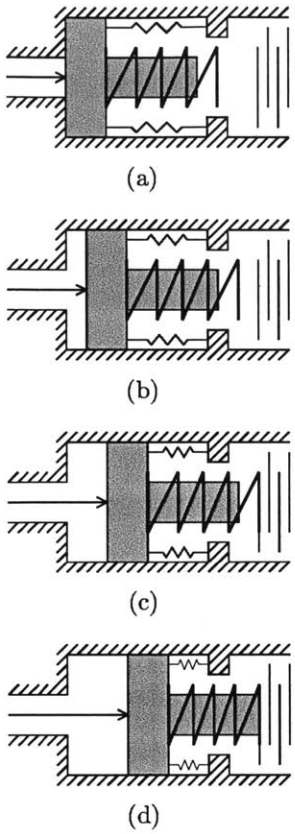

Figure 2-2: A schematic of the clutch actuation: (a) describes Region 1; (b) describes Region 2; (c) describes Region 3; and, (d) describes Region 4. The return spring is the two small outer springs and the isolation spring is the inner spring.

and then fills the clutch accumulator. For this study, we determined experimentally that the dynamics of the variable force solenoid and regulator valve are much faster than the dynamics of the clutch.

2.2.4 Regions of the Shift

We break down the hydraulic clutch actuation into four regions defined by the clutch piston position.

Region 1. The clutch piston is at its maximum distance from the friction plates, x_{max}. Transmission fluid pressurizes the lines and overcomes the return spring preload, while the isolation spring is uncompressed. See Fig. 2-2(a).

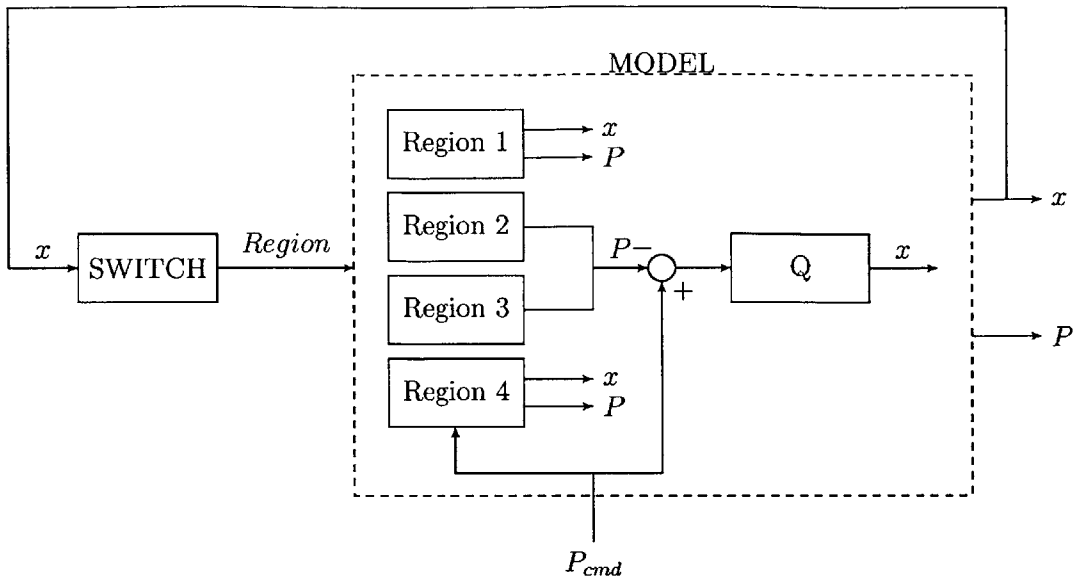

Figure 2-3: Block diagram of the overall clutch model. The region is determined by the clutch piston position x. The commanded pressure P_{cmd} and model parameters are then used to calculate the clutch pressure P as well as the update for the clutch piston position.

Region 2. The transmission fluid fills the clutch accumulator and moves the clutch piston, while compressing the return spring. See Fig. 2-2(b).

Region 3. Transmission fluid continues to fill the clutch accumulator. The isolation spring compresses against the friction plates as the clutch piston continues moving. For a power-on upshift, the torque transfer phase typically begins and the clutch gains some torque capacity against the slipping friction plates. See Fig. 2-2(c).

Region 4. The clutch piston stops traveling and touches the friction plates. Clutch torque capacity increases as the friction plates continue slipping. The clutch pressure and torque capacity can be defined linearly. Within this region, the torque transfer phase will cease and the inertia transfer phase will also occur. See Fig. 2-2(d).

2.3 System Identification Model

Since the clutch piston position may not be known, a system identification model between the commanded pressure and experimentally measured output pressure is

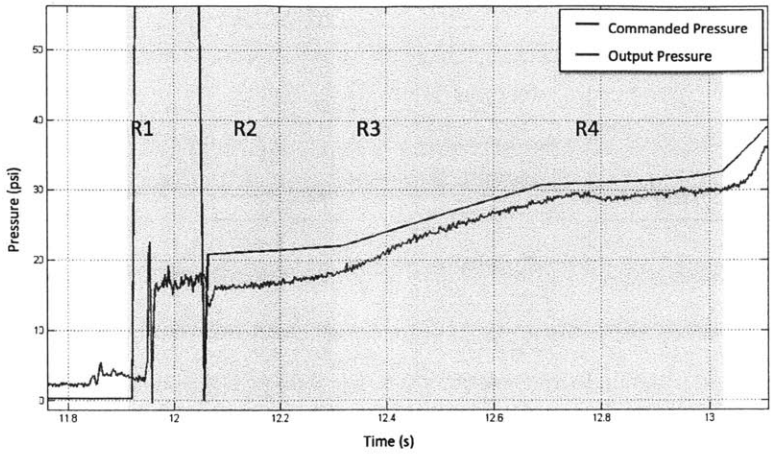

Figure 2-4: Regions of the shift roughly indicated without knowing the clutch piston position. R1, R2, R3 and R4 denote Regions 1 through 4, respectively.

determined. Without knowing the clutch piston position, the regions are roughly indicated in the pressure domain as in Fig. 2-7. This figure illustrates a typical control strategy. The boost phase pressurizes the line (Region 1) and causes the pressure response to get close to stroke pressure. Following the boost phase, a calibrated stroke pressure is commanded. The commanded slope increases once the controller (in open-loop) believes the clutch has gained torque capacity. The final slope (end of Region 4) is commanded via closed-loop control when the speed measurements become available.

To model the output clutch pressure behavior, transfer functions are fitted to the output response in the respective regions.

Regions 1 and 2. The model for Regions 1 and 2 is a combination of a first order low pass filter and an integrator. The low pass filter characterizes Region 1 and the integrator characterizes Region 3. The actual response of Region 1 is a second order system if it were allowed to continue building pressure witl the clutch piston remained fixed. Since the true response of Region 1 leaves too much room for error when switching to Region 2, this combination allows for easier tuning since one less region switching would be needed.

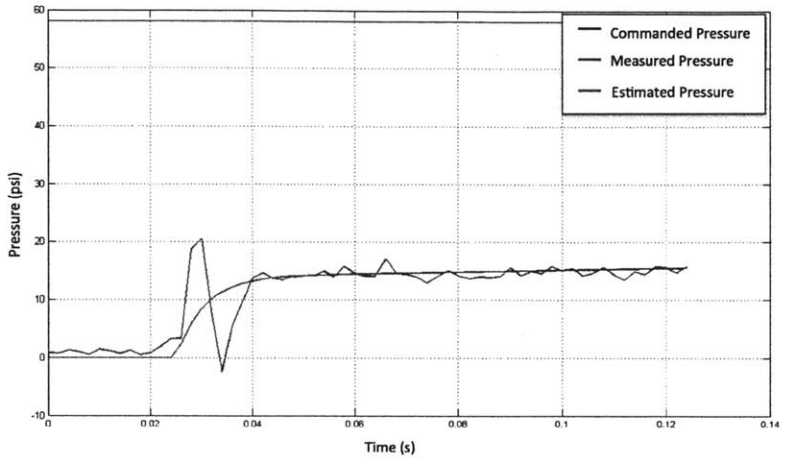

Figure 2-5: Input/output response and model for Regions 1 and 2.

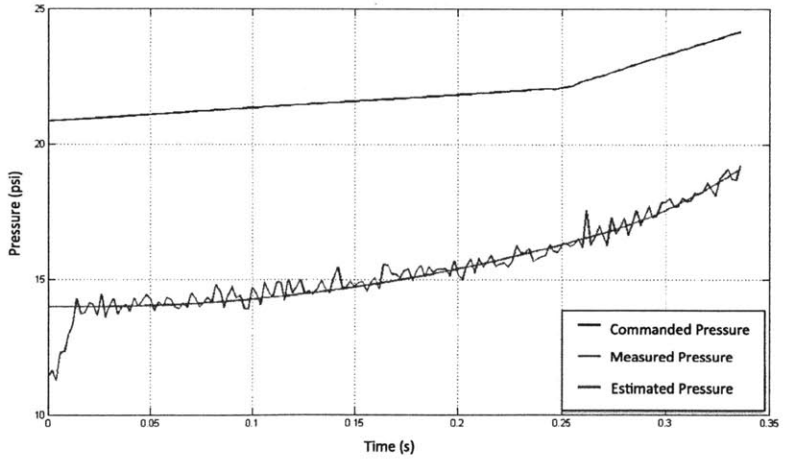

Figure 2-6: Input/output response and model for Region 3.

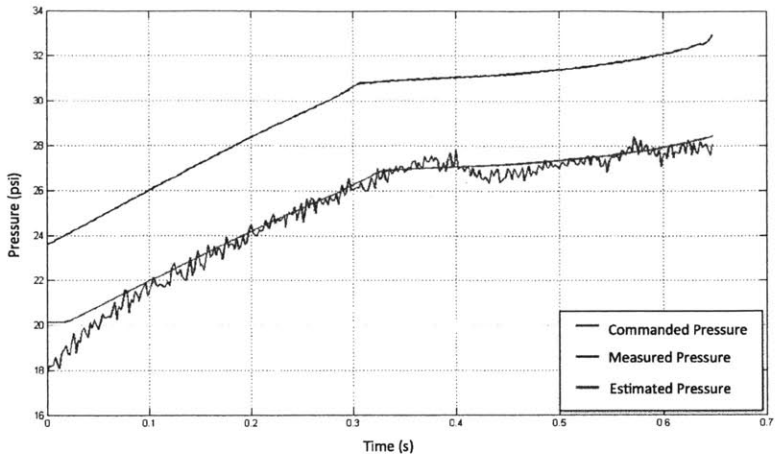

Figure 2-7: Input/output response and model for Region 4.

$$G_{12}(s) = \left(\frac{K_{p1}}{1 + T_{p1}s} + \frac{1}{T_{p2}s}\right) e^{(-T_{d1}s)} \tag{2.1}$$

Region 3. For Region 3, the response is characterized using a second order transfer function. The time constant in this region is much faster than the time constant in the Regions 1 and 2 model.

$$G_3(s) = \left(\frac{K_{p2}}{s(1 + T_{p3}s)}\right) e^{(-T_{d2}s)} \tag{2.2}$$

Region 4. For Region 4, another first order low pass filter is used. The dynamics in this transient are very fast, so the time constant of this model is the fastes of these system identifcation models.

$$G_4(s) = \left(\frac{K_{p3}}{1 + T_{p4}s}\right) e^{(-T_{d2}s)} \tag{2.3}$$

With all of these system identification models, there is a structure of a switching model with different time constants and varying delays. The delay in Regions 1 and 2 is much longer than the subsequent regions because of the delay in pressurizing the hydraulic lines. The time constants inccrease in speed as the model progresses through the regions.

Even though this system identification model is simple and seems to capture the desired transient, it also has many issues. Namely, it is very sensitive to off-nominal conditions, especially the Region 3 model. Also, this model provides no internal state as to when the switching between regions should occur. This model is also very sensitive to error in the region switching. Thus, a model that captures the clutch piston actuation is needed.

2.4 Control-Oriented Model

The control input to the hydraulic clutch system is commanded pressure. The goal of the model is to predict when the clutch strokes based upon history of the commanded pressure. The clutch output pressure is then calculated from the clutch piston position. This is illustrated in Fig. 2-3.

This section begins with the physics-based model, utilized for characterizing Regions 2 and 3, the most important ones for clutch control. The system identification based model of Region 4 is then explained in Section B. In Section C,we explain the modeling procedure used for Region 1.

2.4.1 Physics-Based Model (Regions 2 and 3)

Regions 2 and 3 define the part of the actuation where the clutch piston moves between the bounds of x_{max} and x_0. Using Newtonian dynamics to model the clutch piston movement, we have

$$\ddot{x} = \frac{1}{m}(PA + Kx - F_0 - x_{contact}(x_{free} - x)K_{is} - c\dot{x}) \tag{2.4}$$

such that

$$x_{contact} = \begin{cases} 1 & x \leq x_{free} \\ 0 & \text{otherwise} \end{cases}$$

where $\ddot{x}$ is the clutch piston acceleration, m is the mass of the clutch piston, P is the clutch pressure, A is the cross-sectional area of the clutch apply, K is the return

spring coefficient, x is the clutch piston position, F_0 is the return spring pre-load, $x_{contact}$ is the condition of whether the clutch piston is in Region 2 or Region 3, x_{free} is the height of the isolation spring, K_{is} is the isolation spring coefficient, c is the damping coefficient, and $\dot{x}$ is the clutch piston velocity.

We assume the flow of the transmission fluid through the clutch body is quasi-static. Thus, $\ddot{x}$ and $\dot{x}$ are small, and (2.4) becomes

$$P = \frac{1}{A}(F_0 - Kx + x_{contact}(x_{free} - x)K_{is}) \tag{2.5}$$

Note that when $x = x_{max}$,

$$P = \frac{1}{A}(F_0 - Kx) \tag{2.6}$$

and when $x = x_0$,

$$P = \frac{1}{A}(F_0 + x_{free}K_{is}) \tag{2.7}$$

The solutions of P in (2.6) and (2.7) become the lower bound and upper bound, respectively, of the model output pressure for Regions 2 and 3, which can be used to help tune the initial model parameters.

To relate the control input, u, to the model output pressure, P, we choose the clutch piston position, x, as the state. The clutch piston position is modeled using a flow equation of the pressure drop between the regulator valve and the clutch. The regulator valve is located on the hydraulic line between a variable force solenoid, which provides the commanded pressure, and the clutch body. Assuming there is no saturation of the regulator valve, we have

$$\Delta P = u - P \tag{2.8}$$

$$Q = K_1\Delta P + K_2\sqrt{\Delta P} \tag{2.9}$$

$$x = x_{max} - \frac{1}{A}\int Q\,dt \tag{2.10}$$

where ΔP is the difference in commanded and output pressure, Q is the flow rate, K_1 is the laminar flow coefficient, and K_2 is the turbulent flow coefficient.

The flow coefficients, K_1 and K_2, are most suitable for tuning the model, since the other model parameters are geometric. As K_1 and K_2 vary, the desired output response is tuned. For example, in the case of mostly laminar flow, or low ΔP, the flow coefficients may be chosen to be relatively slow. Also, the ratio of K_1 to K_2 should be considered in order to tune the duration the model is within Region 2 or Region 3.

In summary, the model for Regions 2 and 3 has a single state (x) and two main tuning parameters (K_1 and $K2$). By using information of the clutch piston position, this physics-based model is able to identify the stroke pressure, which is useful for hydraulic control.

2.4.2 System Identification Model (Region 4)

When the clutch piston no longer travels, the dynamics of the hydraulic actuation system are no longer present. The pressure response to command is almost instantaneous, and can be represented by a first order lag with a time delay. We then look to using system identification to fit the response of the output pressure to a first order transfer function with a time delay.

$$\frac{P}{u}(s) = \frac{1}{1+T_p s} e^{(-T_d s)} \tag{2.11}$$

where T_p is the time constant and T_d is the time delay.

This Region 4 model was identified using experimental data in a black box approach. The delay in the system is a result of a variable force solenoid (vfs) and regulator valve earlier in the hydraulic line, and is accounted for with proper tuning of model parameters in the model of Regions 2 and 3. The parameters of the transfer function are a lumped representation of the faster dynamics from the vfs and regulator valve and are not the focus of this study.

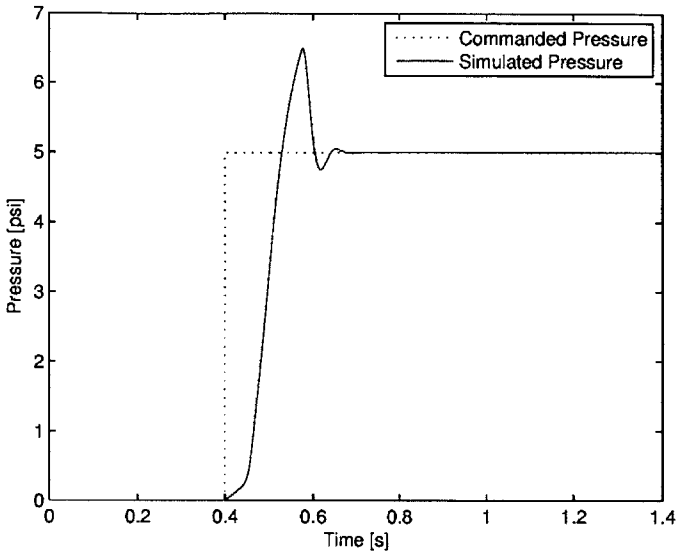

Figure 2-8: Response of hydraulic line pressurizing without the clutch piston moving (Region 1).

2.4.3 Overall Model

Region 1. For the first region, if the clutch piston were held at its maximum position and pressure allowed to build up to a commanded step input, the output pressure would be a second order response as seen in Fig. 2-8. However, the clutch piston moves once the hydraulic pressure overcomes the pre-load of the return spring. As a result, the second order response is interrupted and the actual response for this region looks like an unstable first order response. Therefore, a dynamic model of the true Region 1 response would be difficult to tune and align for the initial condition of Region 2, so we assume the Region 1 model to be constant and defined as

$$P \equiv constant = \frac{1}{A}(F_0 - Kx_{max}) \tag{2.12}$$

Since it is a constant, a time parameter is used to regulate when the overall model will switch from Region 1 to Region 2. From experimental data, the duration of Region 1 was found to be dependent on the temperature of the transmission fluid.

Region 2. Using the condition from (2.4), $x_{contact} = 0$, and (2.5) becomes

$$P = \frac{1}{A}(F_0 - Kx) \tag{2.13}$$

Region 3. Again, using the condition from (2.4), $x_{contact} = 1$, and (2.5) becomes

$$P = \frac{1}{A}(F_0 + K_{is}x_{free} - (K + K_{is})x) \tag{2.14}$$

where x is defined by (2.10).

Region 4. For completeness, we include (2.11) below

$$\frac{P}{u}(s) = \frac{1}{1 + T_p s} e^{(-T_d s)}$$

where x is defined by (2.10).

In summary, the overall model is described by (2.11) through (2.14). It can be seen that the model is of low order, and in Regions 2 and 3 the pressure output model consists of one state: the clutch piston position, x. The model also has two main tuning parameters, K_1 and K_2, for the hydraulic actuation. There is also a time delay in the system modeled in Region 4.

2.5 Model Validation & Analysis

Using a rear-wheel drive passenger vehicle with a six-speed automatic transmission, experimental data of several shift scenarios at various pedal positions were collected.

The baseline shift consists of a boost phase, where a high commanded pressure is used to get close to stroke pressure. The stroke pressure is the pressure needed to fill the clutch body with transmission fluid and compress the return spring before the clutch gains torque capacity. Once the boost phase is complete, the stroke pressure is commanded at a small positive slope to ensure the clutch body continues to fill with transmission fluid. The commanded pressure slope increases when the clutch is expected to have gained torque capacity. Up to this point (approximately Regions 1 through 3), this baseline pressure profile is all commanded in open-loop in a typical transmission control strategy. Feedback is not available until the inertia transfer

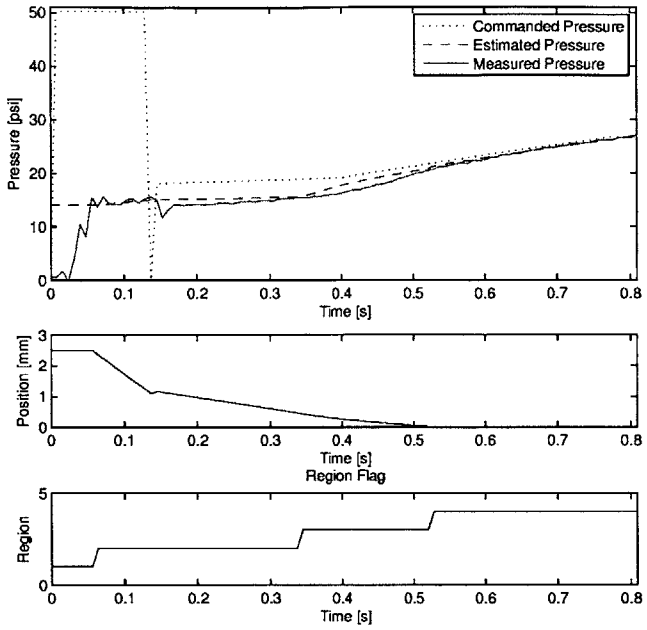

Figure 2-9: Model response to baseline commanded pressure at 10% pedal travel.

phase, which is sometime within Region 4 after the torque transfer phase completes, and a closed-loop control strategy using speed measurements can be used.

The off-nominal shift scenarios are over-boosting, under-boosting, over-stroking, and under-stroking as well as a combination of over-boosting and under-stroking, which are all considered to cause "bad" shifts. Over-boosting means the boost phase is commanded for too long and the clutch strokes completely while commanded pressure is high. The driver experiences this through a large torque disturbance to the vehicle. Under-boosting means the boost phase is not commanded long enough, and the shift will take longer than desired because the clutch accumulator will fill at a low commanded pressure. Over-stroking means the stroke pressure is commanded too high; leading to a rapid start of the torque ratio change. Under-stroking means the stroke pressure is commanded too low and the shift will take longer than desired and causes an increase in engine speed.

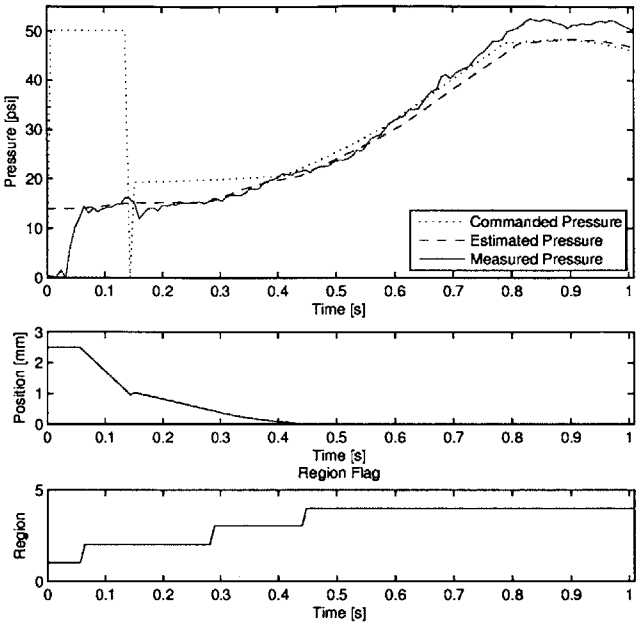

Figure 2-10: Model response to baseline commanded pressure at 60% pedal travel.

2.5.1 Using Nominal Conditions

The first shift scenario is a baseline run using nominal conditions to represent a typical shift as described above. The baseline runs were collected at 10, 15, 20, 25, 30 and 60 percent pedal travel. The 10% and 60% baseline runs are shown in Fig. 2-9 and 2-10, respectively. Qualitatively, we see the estimated output pressure of the model follows very closely with the measured clutch pressure for both low and high throttle commanded pressures. Aside from choosing the parameters A, F_0, K, K_{is}, x_{max}, and x_{free} to coincide with transmission measurements, K_1 and K_2 were tuned for high pressure drop, ΔP, to account for turbulent flow when filling the clutch body with transmission fluid. We also tuned a separate set of K_1 and K_2 for when the clutch empties some of the transmission fluid after the boost phase. The emptying K_1 and K_2 were tuned to be slower than filling since the transmission used to collect vehicle data has a ball-check valve used to slow the flow of transmission fluid when releasing the clutch piston.

Table 2.1: Root mean squared error (RMSE) of the estimated pressure and measured pressure, excluding Region 1.

Shift Scenario	RMSE (psi)
10% Baseline	0.8237
60% Baseline	2.3213
25% Over-boost & under-stroke	3.6040

Looking at the region flag, it can be seen that according to the model, the clutch has stopped stroking and has gained torque capacity well before the commanded pressure changes slope for both baseline experimental runs. The root mean squared error (RMSE) of the estimated pressure and measured pressure are shown in Table 2.1 to quantitatively show how well the model matches the experimental data. Some discrepancy is expected since the measured pressure is sensed sooner in the hydraulic line right outside the clutch body. Also, the commanded pressure shown in the figures is scaled to account for the gain between the commanded pressure and measured pressure, where there should be a 1:1 ratio in Region 4.

2.5.2 Using Off-Nominal Conditions

In order to test the validity of the model, we also conducted shift scenarios where the commanded pressure is over-boosted, under-boosted, over-stroked, under-stroked as well as a combination of over-boosted and under-stroked. The worst case scenario is the combination of over-boosted and under-stroked commanded pressure, which is shown in Fig. 2-11. A first order low pass filter is added to the model so that the transition from Region 4 to Region 3 after boosting is physically realistic. Otherwise, without the filter, the model pressure response would drop from the steady-state pressure of around 50 psi to the upper bound pressure of Region 3 defined by (2.7).

Even though Table 2.1 shows a relatively large error compared to the nominal shift scenarios (mostly because of measurement noise from the over-boost), it is interesting to note how the model captured the return to Region 2 after the boost phase because of the under-stroked pressure command.

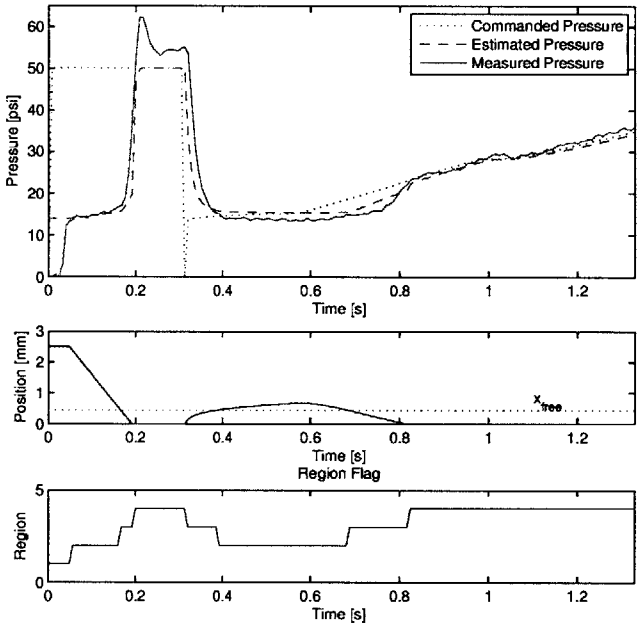

Figure 2-11: Model response to over-boosted and under-stroked commanded pressure profile at 25% pedal travel.

2.6 Summary

In order to run a dynamic clutch model on-board in real time, it should not be computationally intensive, like existing high-fidelity simulation models. Additionally, in order to adequately predict the transients in the clutch body in off-nominal conditions, the model needs to capture the dominant physical phenomena governing the movement of the clutch piston. To address this need, we have developed a simple, one-state model with two main tuning parameters and demonstrated that it is very robust in both nominal and off-nominal testing conditions. Using a combination of physics-based and system identification models, the model is able to maintain details of the clutch actuation, such as identifying the stroke pressure.

The clutch model determines the movement of the piston as a result of the force balance between the clutch pressure, driven by the hydraulic flow from the lines, and the spring forces. This transient spans Regions 2 and 3 as seen in Fig. 2-2. The initial pressurization in Region 1 is sufficiently captured with the assumption of constant pressure. A system identification model successfully represents the fast dynamics of Region 4, which has additional feedback information.

The purpose in developing this model is for its use in automotive control applications. Since current power-on upshift control strategies cannot take advantage of closed-loop control until the inertia transfer phase, or, at best, the torque transfer phase (beginning of Region 3) with clutch torque measurements or estimates, this model aims to aid in the open-loop control of the clutch actuation of Regions 1 through 3. Using the clutch piston position, for example, a hydraulic clutch control strategy may be able to identify the stroke pressure and apply this information to shape the boost phase or commanded stroke pressure in order to improve the quality of the shift and extend the clutches lifespan. The work presented in this chapter has been submitted for publication at the 52nd IEEE Conference on Decision and Control [15].

Chapter 3

Closed-Loop Adaptive Control Design

3.1 Introduction

Using the control-oriented model detailed in Chapter 2, a multi-rate controller is designed to address the overall goals of the project. The main challenge in this project is insufficient feedback information for consistent shifts under all operating conditions. That is, feedback information is not available until the inertia phase when speed measurements start reflecting the shift dynamics. Using measurements or estimates of the shaft torque [18], the clutch torque can be calculated. This calculated clutch torque allows for additional feedback information earlier in the shift (i.e. torque transfer phase), and as will be shown in this chapter, it allows for just enough information to properly tune the hydraulic clutch actuation model using parameter adaptation.

In this chapter, the overall control scheme is outlined in Section 3.2. The parameter adaptation of the hydraulic clutch actuation model is detailed in Section 3.3. Section 3.4 presents the open-loop control design that allows for adaptation "within-the-shift." A summary of this chapter is provided in Section 3.5.

3.2 Overall Control Scheme

The developments in this work focus on power-on shifts, as described in section 2.2.1. In a typical ydraulic clutch actuation control strategy, calibrated parameters shape the open-loop pressure commands until speed signals start changing. Two main parameters, boost time and stroke pressure of the ONC clutch, are used in the initial stages of the shift, when feedback is not available. Thus, there is no real-time adjustment of these parameters that takes place within the same shift. The control scheme presented here utilizes the control-oriented clutch model presented in the previous chapter for real-time adaptation of the boost time and stroke pressure "within-the-shift." The hydraulic clutch actuation model provides estimates of the clutch pressure and clutch piston position, which are used to facilitate the "within-the-shift" adaptation of the boost time and stroke pressure.

3.2.1 Control Structure

The full proposed adaptive strategy is grouped into three update rates

$$\theta_0(n) = \theta_0(n-1) + f_0(e_{t_{23}}, e_{t_{34}}) \tag{3.1}$$

$$\theta_1(k) = \theta_1(k-1) + f_1(e_x) \tag{3.2}$$

$$\theta_2(t) = \theta_2(t-1) + f_2(e_\tau, e_\omega) \tag{3.3}$$

where

$$\theta_0 = \{K_1, K_2, F_0, x_{max}, x_{free}, K, K_{is}, A, T_d, T_p\} \tag{3.4}$$

$$\theta_1 = \{\epsilon_s, P_s, s_2\} \tag{3.5}$$

$$\theta_2 = \{s_3, s_4\} \tag{3.6}$$

$\underline{\theta_0(n)}$: The parameters in θ_0 include all of the hydraulic clutch actuation model parameters. As the update law (3.1) indicates, feedback information of $e_{t_{23}}$ and $e_{t_{34}}$ are used to determine how much the model parameters will change, where $e_{t_{23}}$ and $e_{t_{34}}$

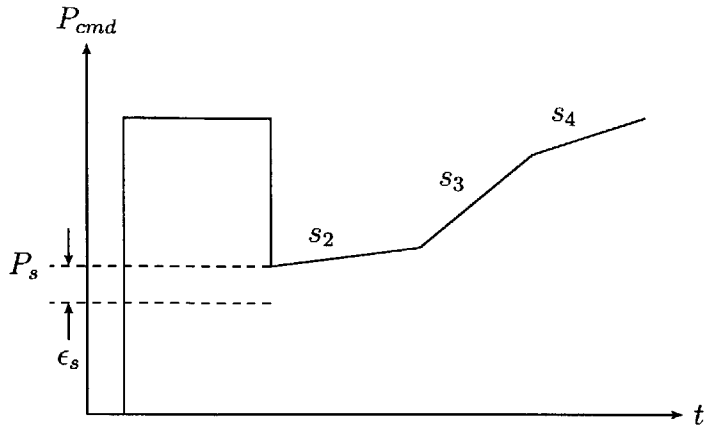

Figure 3-1: Visual explanation of the parameters in the control scheme.

are provided by shaft torque measurements or estimation.

$\theta_1(k)$: Using the estimate of the clutch piston position, the parameters of θ_1 will update accordingly as seen in (3.2). These parameters help shape the clutch command profile used for the open-loop control of Regions 1 and 2. Further details are explained in Section 3.4.

$\theta_2(t)$: Feedback from the shaft torque measurements or estimates and speed measurements are used to update the parameters of the closed-loop control in Regions 3 and 4 as indicated in (3.3). The details of the closed-loop control of these parameters are not included in this thesis. However, the closed-loop control of these regions would be PI controllers for each respective "slope". Meaning, slope s_3 is the closed-loop commanded pressure that meets the target of a smooth torque ratio change. Similarly, slope s_4 is the closed-loop commanded pressure that meets the target of a smooth speed ratio change.

3.2.2 Multi-Rate Update Problem

The three update rates are n, k and t as illustrated in Fig. 3-2. Update rate n is the slowest and includes the model parameters that will update after a certain number of shifts. The update rate k represents each shift. The fastest update rate t is for every time step instance in a shift. The control structure presented here updates at

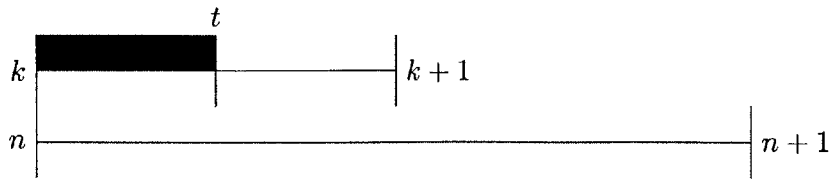

Figure 3-2: Illustration of multi-rate update structure.

various rates because of the complexity of the structure. It is possible because each of the parameter vectors θ_i, $i = \{0, 1, 2\}$, can be updated independent of each other.

3.3 Parameter Adaptation

This section details the parameter adaptation of the hydraulic clutch actuation model, which are the parameters of θ_0. As mentioned in Chapter 2, the main tuning parameters of the model are the lumped flow parameters, K_1 and K_2. All of the other model parameters are not expected to change much over a long period of time with the exception of the main spring pre-load F_0. Therefore, the parameter adaptation and update of θ_0 will focus on K_1, K_2 and F_0 as they contribute the most in the model dynamics.

From (3.1), we will use the feedback information of $e_{t_{23}}$ and $e_{t_{34}}$ to update these three model parameters. The feedback signals are defined by

$$e_{t_{23}} = \hat{t}_{23} - t_{23} \tag{3.7}$$

$$e_{t_{34}} = \hat{t}_{34} - t_{34} \tag{3.8}$$

where the hat terms are the transition time as indicated by the model and the non-hat terms are determined by measurements.

In other words, we assume there is a smooth, nonlinear mapping between the feedback information, $e_{t_{23}}$ and $e_{t_{34}}$, and the model parameters from θ_0: K_1, K_2 and F_0. As Fig. (3-3) shows, this can be written as

$$e(n) = S(\hat{u}(n)) \tag{3.9}$$

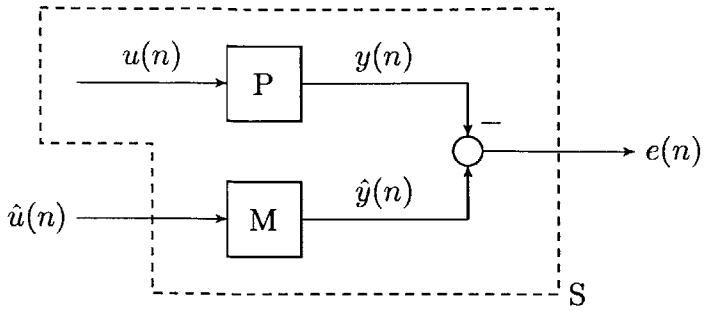

Figure 3-3: Block diagram of model parameter input to error output mapping.

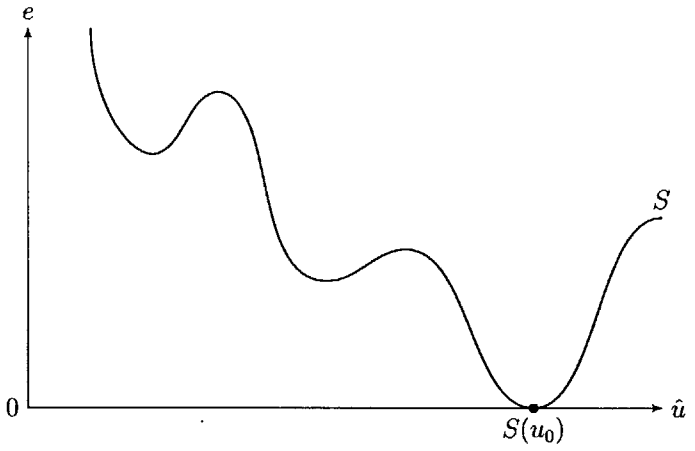

Figure 3-4: Example of nonlinear mapping S.

where

$$e(n) = \begin{bmatrix} e_{t_{23}} \\ e_{t_{34}} \end{bmatrix}, \quad u(n) = \begin{bmatrix} K_1 \\ K_2 \\ F_0 \end{bmatrix} \quad \text{and} \quad \hat{u}(n) = \begin{bmatrix} \hat{K}_1 \\ \hat{K}_2 \\ \hat{F}_0 \end{bmatrix}. \tag{3.10}$$

The goal is thus for $\hat{u}$ to converge to u_0 such that

$$S(u_0) = 0 \tag{3.11}$$

That is we wish to adjust $\hat{u}$ such that $(e(n), \hat{u}(n))$ converges to the equilibrium point $E_0 = (0, u_0)$ as shown in Fig. (3-4). The difficulty that arises is that u_0 and therefore this equilibrium point E_0 is not known and therefore a standard approach based on

linearization of (3.9) around E_0 is not possible. We therefore define

$$\Delta\hat{u}(n) = \hat{u}(n) - \hat{u}(n-1) \tag{3.12}$$

$$\Delta e(n) = e(n) - e(n-1) \tag{3.13}$$

and express a linearized relation

$$\Delta e(n) = J(n)\ \Delta\hat{u}(n) \tag{3.14}$$

where the Jacobian $J(n)$ is defined as

$$J(n) = \left[\frac{\partial e_i}{\partial \hat{u}_j}\right] \text{ for } (\hat{u}_j(n), e_i(n)), j = \{1,2,3\}, i = \{1,2\}$$

Assuming that $J(n)$ is known, the relation (3.14) is used to determine $\hat{u}$ at $n+1$ in teh following manner: Given $e(n)$ and $\hat{u}(n)$, since our goal is to drive e to zero, we will attempt to find $\hat{u}$ atthe next instant of time, $n+1$, such that $e(n+1) = 0$. That is, $\hat{u}(n+1)$ must satisfy the condition

$$J(n+1)[\hat{u}(n+1) - \hat{u}(n)] = -e(n) \tag{3.15}$$

This can be restated as the solution of the optimization problem

$$\min_{\Delta\hat{u}(n+1)} ||J(n+1)\Delta\hat{u}(n+1) + e(n)||_2^2 \tag{3.16}$$

If a solution exists for (3.16), then this implies that we have determined the ideal step that $\hat{u}$ that has to change by in order to bring the trajectories of $\hat{u}$ and e to the equilibrium point E_0. A numerical procedure based on the active set method [7] is used in order to find the solution to (3.16).

In the above problem statement, we have assumed that J is known, or that it can be constructed by estimating the underlying gradients. In order to improve the accuracy of J, we propose the use of a Kalman filter, which is described below.

3.3.1 Estimation of J using a Kalman Filter

Assuming J can be modeled with fictitious noise and linear dynamics, the structure of (3.17) can be used to minimize w_j, the imprecision of the linearized model (3.14) with covariance $Q_j = E\{w_j^T(n)w_j(n)\}$, and v_j, measurement noise with zero mean and variance $R_j = E\{v_j^2(n)\}$. This structure allows the application of a Kalman filter to learn the true Jacobian. For the completeness of this thesis, the Kalman filter detailed in [3],[11],[4] is included and adapted to this problem: To use the Kalman filter for learning, we decompose the multi-input multi-output linearized system (3.14) into three multi-input single-output subsystems $\Delta e_j(n+1) = J_j^T(n+1)\Delta\hat{u}(n+1), j = \{1,2,3\}$, where J_j^T is the jth row of the Jacobian J.

$$\begin{aligned} J_j(n+1) &= J(n) + w_j(n) \\ \Delta e_j(n) &= \Delta\hat{u}^T(n)J_j(n) + v_j(n), j = \{1,2,3\} \end{aligned} \tag{3.17}$$

The expression used for recursive updating of the rows of the Jacobian estimate of each of the subsystems $\hat{J}_j$ is:

$$\hat{J}_j^T(n+1) = \hat{J}_j^T(n) + \frac{P_j(n)\Delta\hat{u}(n)}{R_j + \Delta\hat{u}^T(n)P_j(n)\Delta\hat{u}(n)}(\Delta e(n) - \hat{J}_j(n)\Delta\hat{u}(n)) \tag{3.18}$$

$$P_j(n+1) = P_j(n) - \frac{P_j(n)\Delta\hat{u}(n)}{R_j + \Delta\hat{u}^T(n)P_j(n)\Delta\hat{u}(n)}\Delta\hat{u}^T(n)P_j(n) + Q_j \tag{3.19}$$

In Filev's work [5],[3], he presents an alternative to using the Kalman filter via Least Mean Squares (LMS). Using LMS, the expression for updating the Jacobian estimate is:

$$\hat{J}^T(n+1) = \hat{J}_j^T(n) + \alpha\frac{[\Delta e(n) - \hat{J}(n)\Delta\hat{u}(n)]\Delta\hat{u}^T(n)}{\Delta\hat{u}^T(n)\Delta\hat{u}(n)} \tag{3.20}$$

where $0 < \alpha < 2$ is the learning rate.

In this work, the LMS (3.20) method was not used because the convergence of the Jacobian is sensitive to proper selection of the learning rate α. In choosing to use the Kalman filter (3.18-3.19), the sensitivity decreases because the learning rate is essentially determined by the covariance matrix P_j.

Filev's works also compare the Kalman filter to the Recursive Least Squares (RLS) algorithm. To illustrate the subtlety in the difference between these algorithms, both the RLS and RLS with forgetting factor algorithms [12] are shown below.

RLS:

$$\hat{J}_j^T(n+1) = \hat{J}_j^T(n) + \frac{P_j(n)\Delta\hat{u}(n)}{I_j + \Delta\hat{u}^T(n)P_j(n)\Delta\hat{u}(n)}(\Delta e(n) - \hat{J}_j(n)\Delta\hat{u}(n)) \tag{3.21}$$

$$P_j(n+1) = P_j(n) - \frac{P_j(n)\Delta\hat{u}(n)}{I_j + \Delta\hat{u}^T(n)P_j(n)\Delta\hat{u}(n)}\Delta\hat{u}^T(n)P_j(n) \tag{3.22}$$

RLS with forgetting factor:

$$\hat{J}_j^T(n+1) = \hat{J}_j^T(n) + \frac{P_j(n)\Delta\hat{u}(n)}{\lambda + \Delta\hat{u}^T(n)P_j(n)\Delta\hat{u}(n)}(\Delta e(n) - \hat{J}_j(n)\Delta\hat{u}(n)) \tag{3.23}$$

$$P_j(n+1) = \frac{1}{\lambda}\left[P_j(n) - \frac{P_j(n)\Delta\hat{u}(n)}{\lambda + \Delta\hat{u}^T(n)P_j(n)\Delta\hat{u}(n)}\Delta\hat{u}^T(n)P_j(n)\right] \tag{3.24}$$

where λ is the forgetting factor.

In the Kalman filter, the covariance Q_j acts as a drift factor and is analogous to the forgetting factor λ in the RLS algorithm. The drift factor has two advantages over the forgetting factor: (i) If the system is not excited, the drift factor allows the covariance matrix to grow linearly as opposed to exponentially with the forgetting factor; (ii) If some of the estimated parameters change more than others, the drift factor can account for this, while the forgetting factor weighs on all of the parameters equally.

Now that $J(n+1)$ is known, we can return to (3.14) and see that we have

$$e(n+1) - e(n) = J(n+1)\Delta\hat{u}(n+1) \tag{3.25}$$

The main component of the learning algorithm proposed in this thesis is the optimization problem stated in (3.16). We propose the use of the active set method [7] to solve this problem. This method is described in further detail below.

3.3.2 Implementation of Algorithm

We rewrite (3.16) as

$$\begin{aligned} &\min_x \frac{1}{2} x^T H x + c^T x \\ &\text{subject to } Ax \leq b \text{ and } l \leq x \leq u \end{aligned} \tag{3.26}$$

where x is the optimizer and

$$H = \begin{bmatrix} I \\ J(n+1) \end{bmatrix} \text{ and } c^T = \begin{bmatrix} 0 \\ e(n) \end{bmatrix}.$$

This means we have a quadratic programming problem subject to linear constraints. The Matlab Optimization Toolbox function `lsqlin()` uses a null space active set method for this situation of mixed inequatlity constraints ($Ax \leq b$) and bounds ($l \leq x \leq u$), and references the work of Gill [6],[7],[8]. The solution to (3.26) will be the update for goal of (3.16).

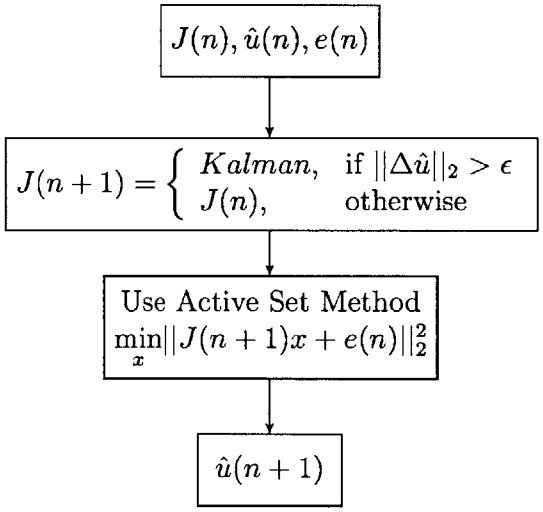

Figure 3-5: Data flow of indirect parameter adaptation.

3.3.3 Robustness Analysis of Parameter Adaptation

To test the robustness of the parameter adaptation, both nominal and off-nominal vehicle parameters are used in a simulated high-fidelity vehicle dynamics and hydraulic

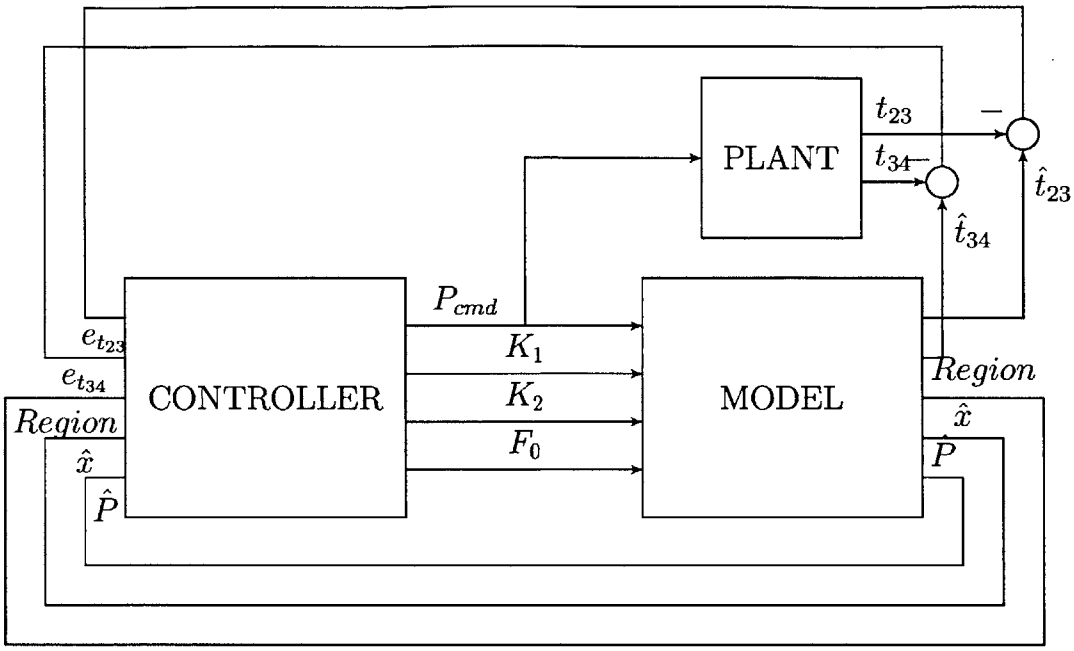

Figure 3-6: High level representation of the proprietary Ford model used for simulation.

clutch system model in Matlab Simulink as seen in Fig. (3-6). The high-fidelity model functions as the "plant" in this analysis. The controller in the simulation commands the pressure to both the plant and the model, and the details of this controller are presented in Section 3.4.

In this analysis, the parameters K_1, K_2 and F_0 started at 25 different initial conditions and were allowed to adapt. The initial conditions chosen were a sweep of K_1 and K_2 values within their respective physical bounds, while F_0 was initiliazed to its known nominal value.

Using Nominal Conditions

As Fig. 3-7 illustrates, the adaptation algorithm performed very well. The goal of minimizing the errors in t_{23} and t_{34} was met. After running all of the initial conditions using nominal transmission parameters, 56% of the adaptation runs successfully converged and met the error target. As mentioned above and shown in Fig. 3-4, it is expected that because the Jacobian is a linearization of the nonlinear mapping (3.9)

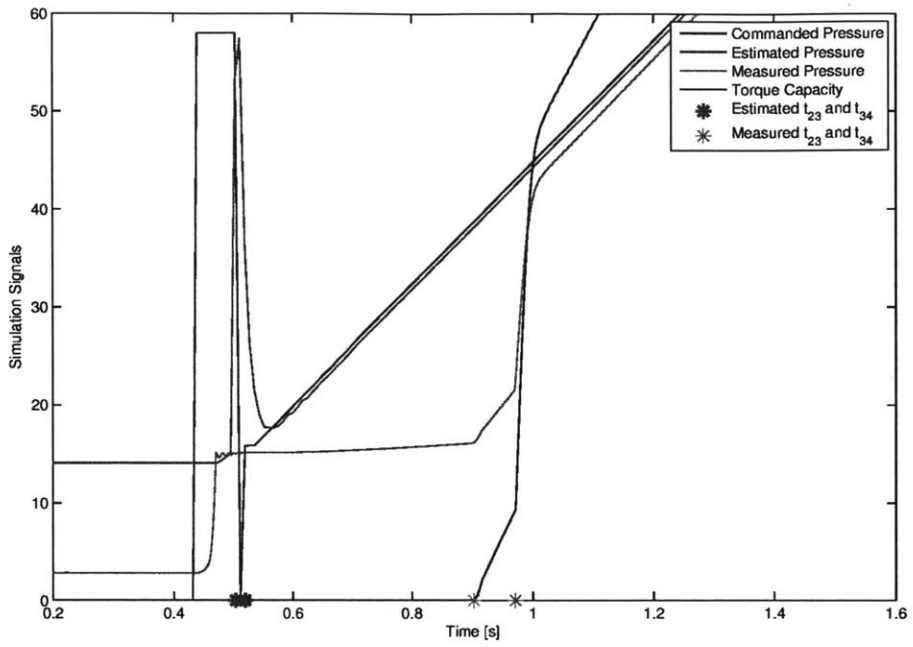

(a)

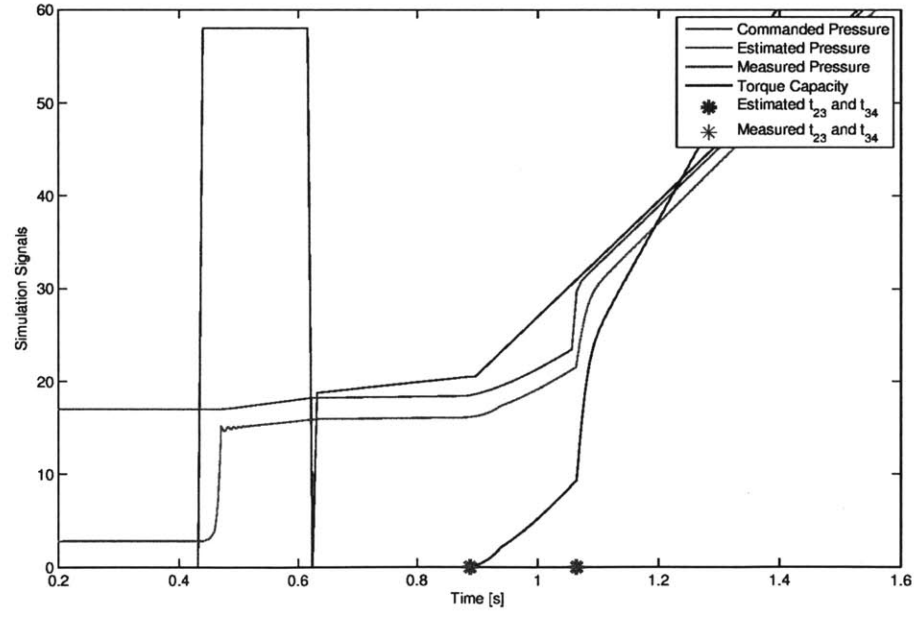

(b)

Figure 3-7: Nominal conditions comparison of (a) first shift using initial condition and (b) final converged shift using adapted values.

that the adaptation may reach a local minimum. Also, it is noted that some of the initial conditions did not allow for any adaptation, which is also expected according to the conditions of the active set method. In either of these cases, successful convergence of the parameter adaptation and minimization of the error target can still be achieved by re-initializing the Jacobian using the underlying gradients in the new parameter space. That is, the idea is to use the failed K_1 and K_2 adapted values as new initial conditions and run the adaptive algorithm again. This methodology has proven to be successful in simulation.

Of the runs that successfully converged and met the error targets, the final converged values of K_1 and K_2 seemed to converge close to similar values. This leads to the conclusion that the adaptive algorithm is able to learn the "actual" K_1 and K_2 values. It is important to note that F_0 did not converge to similar values in any runs and merely facilitated additional excitation for the learning algorithm to properly adapt K_1 and K_2 accurately. Since F_0 does not converge to an actual value, a final step in the algorithm will need to be added to account for the offset in the pressure domain that results from an erroneous pre-load value. However, this has not been determined yet and is included in the future work of this project. The findings in this chapter are preliminary and it is still to be determined how exactly the adaptation should be applied such as choice of adaptive parameters, etc.

Using Off-Nominal Conditions

The off-nominal conditions tested are $\pm 10\%$ of x_{max}, x_{free}, K, and K_{is}. However, only the results from x_{max} and x_{free} are included in this thesis. Overall, all of the off-nominal conditions did not deter the parameter adaptation from performing well as shown in Fig. B-4. As expected, the lumped flow parameters K_1 and K_2 were able to account for the discrepancies in the off-nominal conditions by converging 57% of the runs. Of these converged runs, both K_1 and K_2 again converged to similar values signifying convergence to "actual" K_1 and K_2 values.

In summary, the lumped flow parameters K_1 and K_2 as well as the main spring pre-load F_0 of the hydraulic clutch actuation model are used in an adaptive parameter

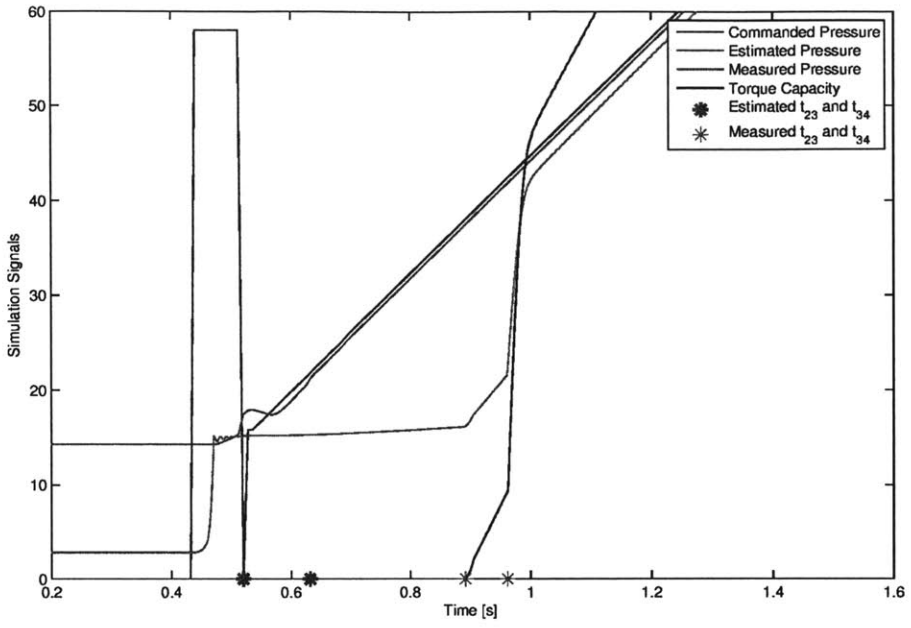

(a)

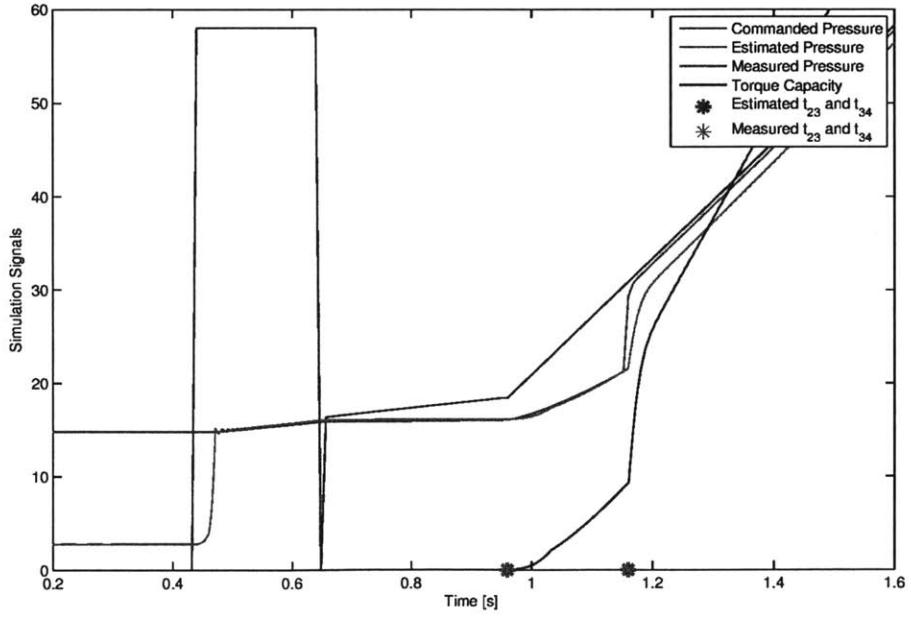

(b)

Figure 3-8: Off-nominal condition of -10% x_{max} comparison of (a) first shift using initial condition and (b) final converged shift using adapted values.

algorithm to minimize the error in the region switching times t_{23} and t_{34}. The times t_{23} and t_{34} are retrieved from a clutch torque signal that is calculated from either shaft torque measurements or estimates. The adaptive algorithm uses a Kalman filter to learn the underlying gradients of the nonlinear mapping between the errors and the adaptive parameters, while the adaptive parameters are optimized using an active set method. The algorithm detailed above has shown to perform well in simulation.

It is important to note that K_1 and K_2 were originally considered as the only adaptive parameters. The Matlab active-set method is a null-space method, so the row dimension of the working set should be as large as possible to help with efficiency of the algorithm. This is because the working set is constructed from the null space of the active constraints. When the number of active constraints increases, the result is a decrease in the dimension of the null space. Thus, the larger the size of the working set, the more efficiently the problem solves [6]. When we originally only considered K_1 and K_2 in the parameter vector x, the working set had a lower row dimension than when using K_1, K_2, and F_0. Qualitatively, only using K_1 and K_2 resulted in a detioriation of the number of converged runs, and made it more difficult to meet the target goal of reducing the errors in t_{23} and t_{34}. Hence, possibly including more of the model parameters into x would be advantageous. However, since the feedback/target are in the time-domain, this may not help because it could cause the response in the pressure domain to become physically unrealistic. Also, increasing the number of model parameters in x may cause the associated matrices to become sparse. Thus, the null-space method would not be useful, since the dimension of the null space will be much larger than the range of the space.

3.4 Open-Loop Controller (Regions 1 and 2)

The open-loop controller uses the parameters of θ_1 to shape the pressure command profile of Regions 1 and 2, and for convenience is listed here:

$$\theta_1 = \{\epsilon_s, P_s, s_2\} \tag{3.27}$$

where ϵ_s is a threshold around the estimated stroke pressure, P_s is the commanded stroke pressure, and s_2 is the commanded slope of the stroke pressure.

3.4.1 Boost Phase Control

A faster hydraulic transient can be achieved by initially commanding significantly higher than desired pressure, also known as "boost phase. Using the hydraulic clutch actuation model, as well as measurements/estimates of the shaft torque to calculate clutch torque, allows real-time determination of when to exit the boost phase. As mentioned earlier, in some hydraulic clutch control algorithms, the boost phase duration is a calibrated value and is not updated until subsequent shifts. Thus, if it is not calibrated correctly or a disturbance to the driveline occurs, the clutch can experience either an over-boost or an under-boost event, which leads to undesirable shift quality. A dynamic boost duration minimizes the possibility of these events from occurring and allows for adaptation "within-the-shift". The dynamic structure of the boost phase control is two-fold consisting of an upper and lower limit.

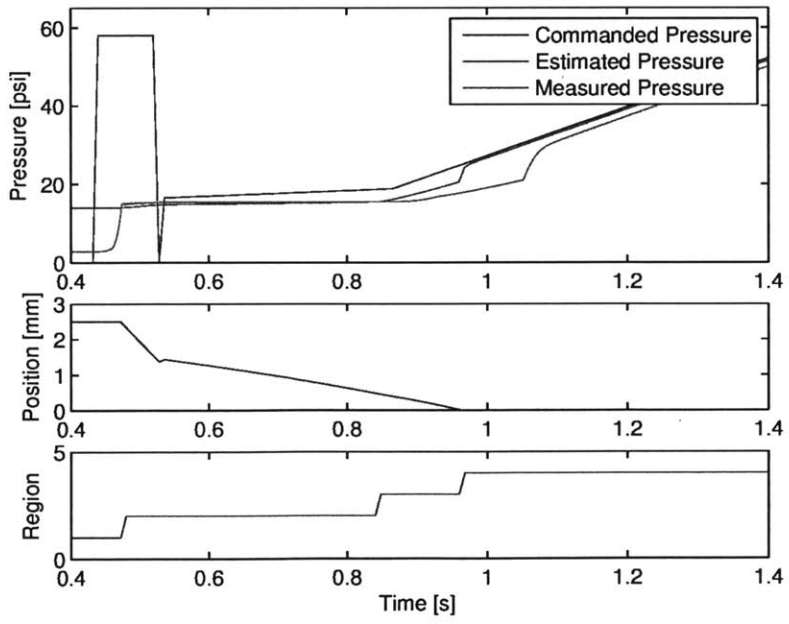

Figure 3-9: Example of the boost phase control.

Upper Limit

Using the calculated clutch torque from either measurements or estimates of the shaft torque allows the system to know when the plant clutch has gained torque capacity, which is also known as t_{23}. The hydraulic clutch actuation system also estimates when the clutch has gained torque $\hat{t}_{23}$. By definition, over-boosting is the boost phase commanding for too long resulting in the clutch gaining torque capacity while still in the boost phase. Since the clutch gaining torque capacity can be detected either via measurements or estimates, t_{23} or $\hat{t}_{23}$, these instances are used as an upper limit to stop the boost phase once they occur. This is considered an upper limit to the boost phase because it prevents over-boosting from occuring, which is maximum amount of time to boost.

Lower Limit

The lower limit uses the θ_1 parameter ϵ_s to help minimize under-stroking from occuring. By setting a threshold under the esimated stroke pressure, it can be used a conservative trigger to stop the boost phase. The purpose of the boost phase is to command a high pressure for as long as possible to help decrease the time spent pressurizing the hydraulic line and get close to the actual stroke pressure. Choosing a small tolerance of the expected stroke pressure creates a lower limit for the amount of boosting. The actual value of ϵ_s can be chosen either as a tolerance in the pressure domain or in the clutch piston position domain. The example in Fig. 3-9 uses the pressure domain by monitoring the estimated output pressure from the hydraulic clutch actuation model until it is within the specificied epsilon of the stroke pressure. A similar example can be shown using the estimated clutch piston position from the hydraulic clutch actuation model to monitor when the clutch is close to the isolation spring and thus close to when the clutch will start gaining torque capacity.

The adapation "within-the-shift" of the boost phase has shown to perform well in simulation. This open-loop control design for the boost phase was also tested against

experimental data of over-boosted and under-boosted shift events. In the cases of over-boosting, this dynamic boost phase would have commanded the boost phase to stop prior than what actually occured in vehicle. Similarly, for the under-boosting cases, this open-loop controller would have commanded longer to get as close as possible to when clutch torque capacity would start gaining.

3.4.2 Stroke Pressure Control

After the boost phase, the stroke pressure is commanded. However, the stroke pressure, i.e. the pressure at which the clutch gains torque transmitting capacity, is not exactly known. In regards to stroking, there are two undesirable shift events: over-stroking and under-stroking. Over-stroking is difficult to detect with the information available on-board a production vehicle, since it is mostly noticeable via a large torque disturbance to the shaft, but other factors can also cause this behavior. Similarly, under-stroking is also difficult to detect, because it is usually evidenced by long shift times as well as overshoot in engine speed. With the hydraulic clutch actuation model, an estimate of the clutch piston position is available. Using this estimate of the clutch piston position, under-stroking is easily detectable.

When under-stroking occurs, the clutch piston starts to de-stroke. In other words, the clutch piston begins to move in the opposite direction intended for the shift. Therefore, the open-loop controller proposed here purposely chooses P_s to be a low value to ensure under-stroking occurs. By monitoring when the clutch piston reverses direction, the control parameter P_s can quickly increase until the clutch piston begins moving in the correct direction again. Thus, adaptation "within-the-shift" is again achieved. The P_s parameter is categorized in θ_1 because this under-stroking technique is used as a learning algorithm for the actual commanded stroke pressure of P_s. More specifically, this under-stroking technique is used for a certain number of shifts and an average of the converged P_s values is then set as the actual P_s value.

Once P_s is done commanding, the slope s_2 is commanded until the clutch gains torque capacity. The slope s_2 is a low ramping of the stroke pressure to ensure the clutch piston continues to stroke until the clutch gains torque capacity. Once torque

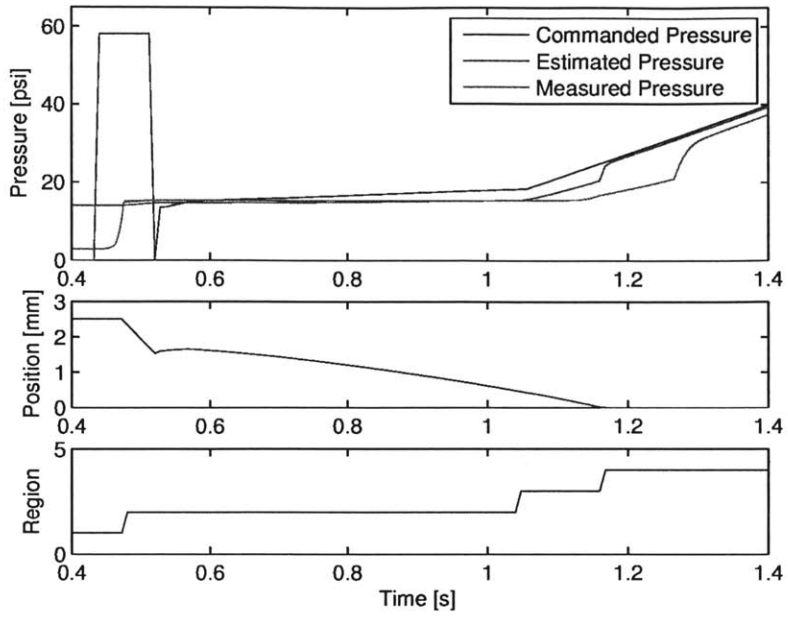

Figure 3-10: Example of the stroke pressure control.

capacity is gained, the closed-loop controller takes over and uses the shaft torque and speed feedback information. An example of this open-loop stroke pressure control is shown in Fig. 3-10.

3.5 Summary

This chapter presented a complex control structure of three various update rates. Each update rate allows for the control of a set of parameters, which are able to update independently of the other rates. The first set of parameters θ_0 are from the hydraulic clutch actuation model and only K_1, K_2 and F_0 are chosen for the parameter adaptation algorithm since they contribute the most to variability in the model. The second set of parameters θ_1 are the parameters of the open-loop controller to shape the command profile for Regions 1 and 2, while θ_2 are the closed-loop controller parameters not detailed in this thesis.

The parameter adaptation used the three model parameters to tune the hydraulic

clutch actuation model to more accurately match the plant dynamics. This was achieved by using the feedback information provided by shaft torque measurements or estimates to calculate the clutch torque capacity. Knowing the clutch torque capacity, the time instances when the clutch first gains capacity t_{23} and when the clutch piston is fully stroked t_{34} can be determined and are thus compared to the models estimate of these values. These errors provided feedback to the adaptation algorithm to learn the underlying gradients of the nonlinear mapping between the model parameters and the errors in order to adjust the model parameters to reduce the error. In simulation, the parameter adaptation algorithm has shown to work very well. Of the successful runs, the converged values of K_1 and K_2 were respectively close to each other, which leads to the conclusion that the actual K_1 and K_2 values were learned. However, F_0 did not converge to similar values, which means an additional method will need to be applied to help compensate for the error in F_0.

The open-loop controller design allows for adaptation "within-the-shift" by properly shaping the pressure command profile despite disturbances or model errors. Typical control strategies use calibrated values of the boost phase duration and stroke pressure. However, using the model and torque information, the boost phase become dynamic and no longer a needed calibration. Additionally, the commanded stroke pressure can be learned using the under-stroking technique, and even the learning shifts perform well since the commanded pressure adjusts throughout the shift.

Overall, the goal of the thesis to adapt "within-the-shift" is met through the use of the hydraulic clutch actuation model and the open-loop controller design.

THIS PAGE INTENTIONALLY LEFT BLANK

Chapter 4

Conclusions and Suggestions for Future Work

4.1 Contributions of this Thesis

This thesis meets the goal of improving the open-loop control design to adapt "within-the-shift" as well as creates a model-based closed-loop adaptive control. To meet these goals, a low order model of the hydraulic clutch actuation was developed by first breaking up the shift dynamics into smaller regions defined by the clutch piston position. In order to avoid issues of switching between first and second order system identification models of these regions, a simplification of the physical equations governing the actuation was produced and validated using nominal and off-nominal experimental data.

Calculated clutch torque is used to tune the hydraulic clutch actuation model via a closed-loop parameter adaptation algorithm. Only three model parameters are needed in the adaptation, and these parameters are the lumped flow parameters K_1 and K_2 as well as main spring pre-load F_0 because they contribute the most to the variations from the plant. The calculated clutch torque allows the identification of the time when the clutch torque gains capacity t_{23} as well as when the clutch piston is fully stroked t_{34}, which are then used as feedback information for the parameter adaptation. An indirect parameter adaptation method using the underlying gradients to map the

behavior between changes in the parameters K_1, K_2 and F_0 and the errors in t_{32} and t_{34} is implemented and shown to perform well in simulation. The underlying gradients are more accurately learned using a Kalman filter and the parameter updates are optimized using an active set method.

Finally, the open-loop control designed in this thesis allows for less stringent calibration as it allows for adaptation during shift of the boost phase and learns the commanded stroke pressure. The boost phase adapts during shift through the monitoring of a lower limit defined by being close to within the estimated stroke pressure and an upper limit defined by the clutch torque gaining capacity. The commanded stroke pressure is learned using an under-stroking technique that involves monitoring the estimated clutch piston position.

All of this is achieved because of the unique ability the model developed in this thesis provides to estimate the clutch piston position and clutch pressure. The control structure presented is able to robustly adapt the model to match the plant dynamics and shape the commanded pressure profile via open-loop because of calculated clutch torque from shaft torque estimates or measurements.

4.2 Suggestions for Future Work

Overall, the proposed control scheme presented in this thesis works very well. However, the parameter adaptation algorithm is not complete in that the main spring preload F_0 does not converge to its true value. Including F_0 in the parameter adaptation was necessary to provide enough information to the system to excite the learning of the lumped flow parameters K_1 and K_2. In simulation, the converged values of F_0 were not the same and spanned the possible values of F_0. This discrepancy in F_0 is not desirable since it largely contributes to the offset in the pressure domain as seen in the estimate of the clutch pressure. Thus, additional work is needed to reduce this error. It is hypothesized that shaft speed measurements may be able to assist in this endeavor since there is a linear relationship between the clutch torque and the clutch pressure when inertial data is available.

It is also noted that the control algorithm presented has only been tested in simulation. To truly demonstrate the capabilities of the algorithm, it will need to be tested on a vehicle via experimentation using nominal and off-nominal shift conditions and vehicle parameters. Additionally, the closed-loop control of Regions 3 and 4 using shaft torque measurements is to be completed and tested on vehicle.

Furthermore, it is postulated that the hydraulic clutch actuation model is not only beneficial to model the application of the on-coming clutch, but the release of the off-going clutch as well. It has not been determined whether adaptation will be able to occur on the release-side as well as the apply-side or whether adaptation will solely occur on the apply-side. Also, identification of the shift regions on the release-side is not as straightforward at this time and will need further examination.

THIS PAGE INTENTIONALLY LEFT BLANK

Appendix A

More Model Validation Results Using Off-Nominal Conditions

A.1 Over-boost

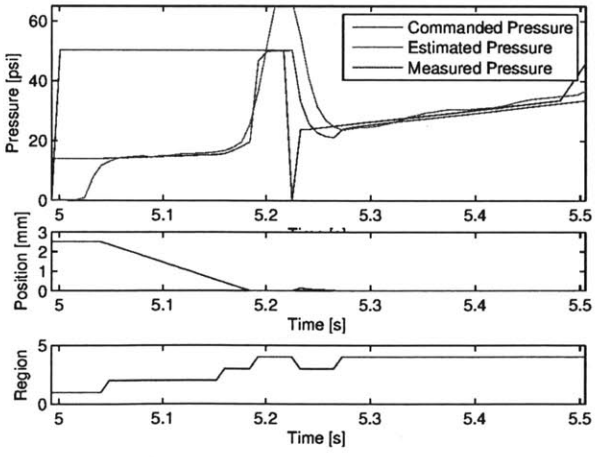

Figure A-1: Example of over-boost from 10% pedal command.

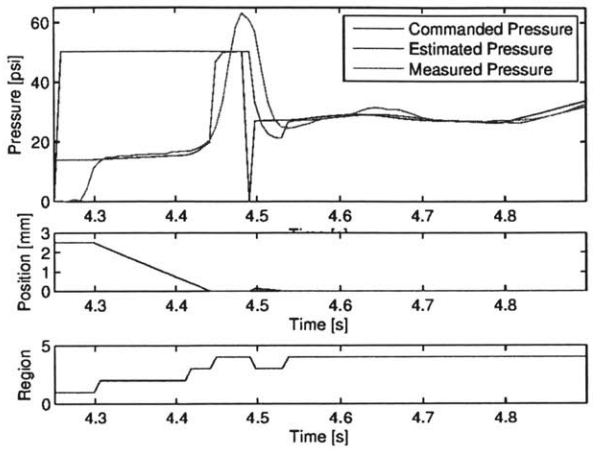

Figure A-2: Example of over-boost from 15% pedal command.

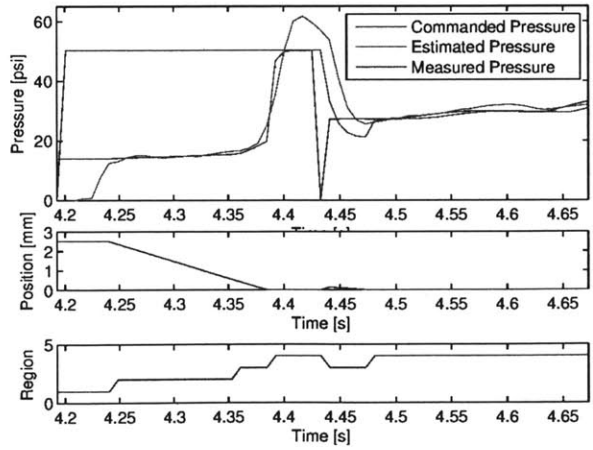

Figure A-3: Example of over-boost from 20% pedal command.

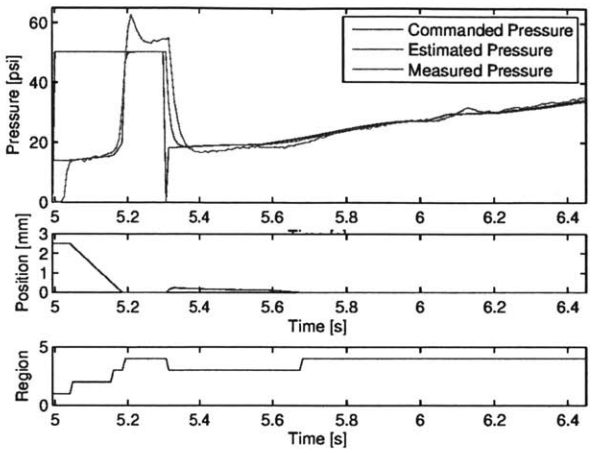

Figure A-4: Example of over-boost from 25% pedal command.

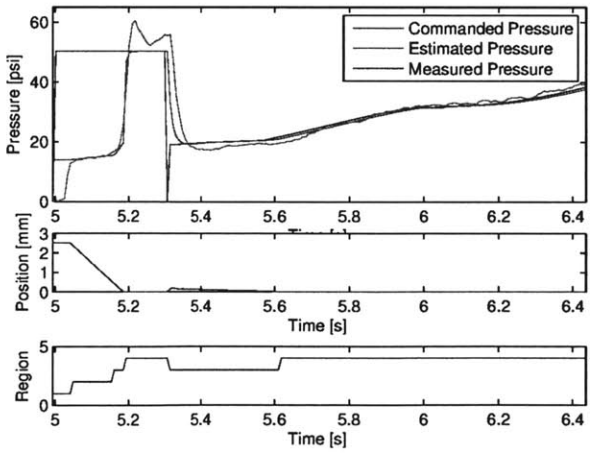

Figure A-5: Example of over-boost from 30% pedal command.

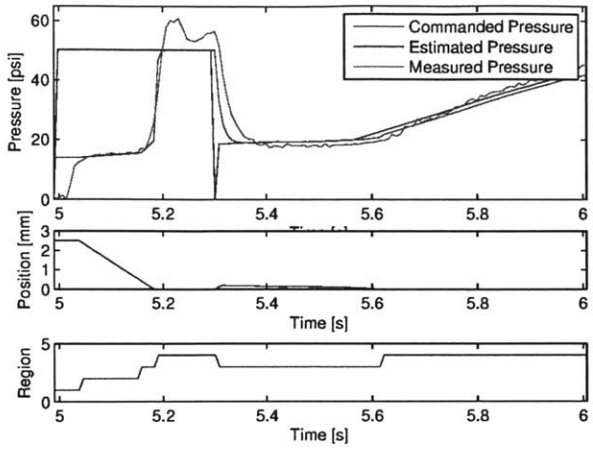

Figure A-6: Example of over-boost from 60% pedal command.

A.2 Under-boost

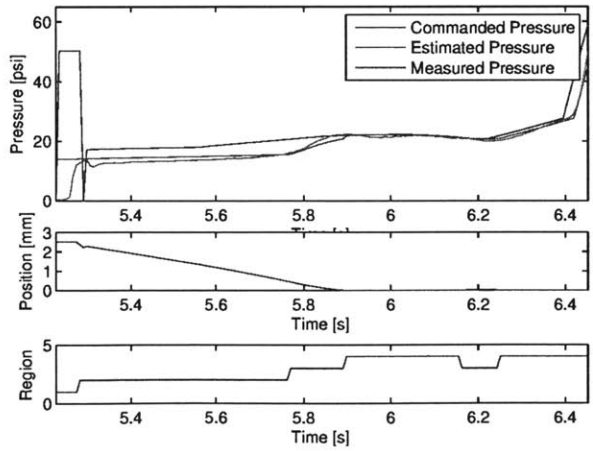

Figure A-7: Example of under-boost from 10% pedal command.

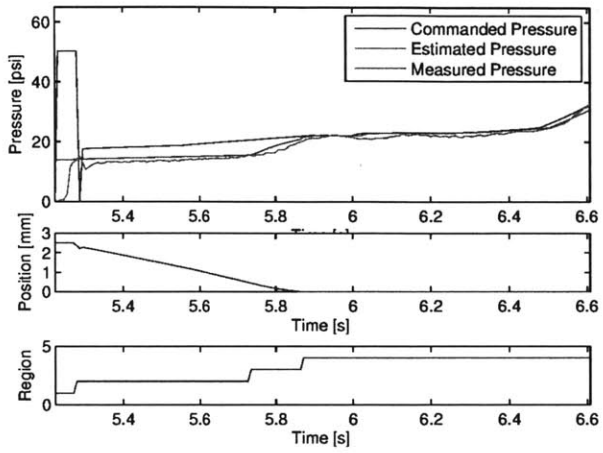

Figure A-8: Example of under-boost from 15% pedal command.

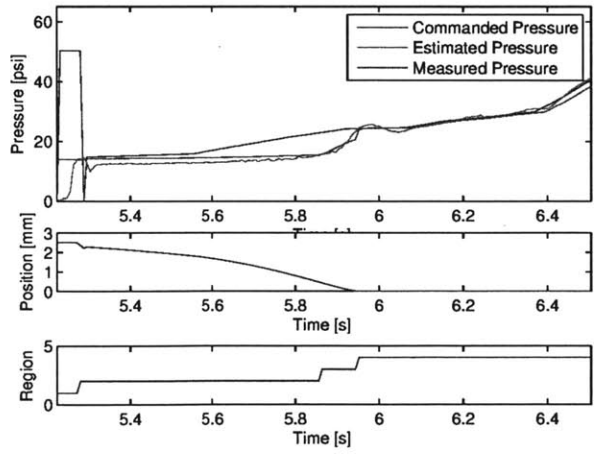

Figure A-9: Example of under-boost from 20% pedal command.

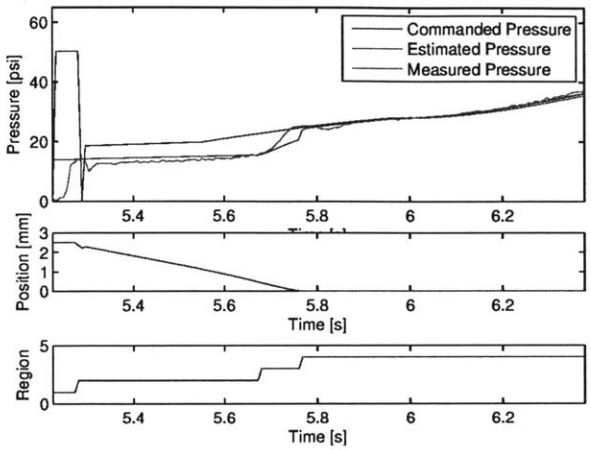

Figure A-10: Example of under-boost from 25% pedal command.

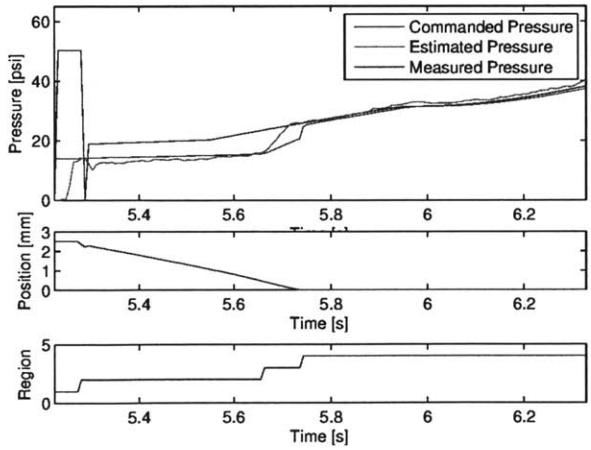

Figure A-11: Example of under-boost from 30% pedal command.

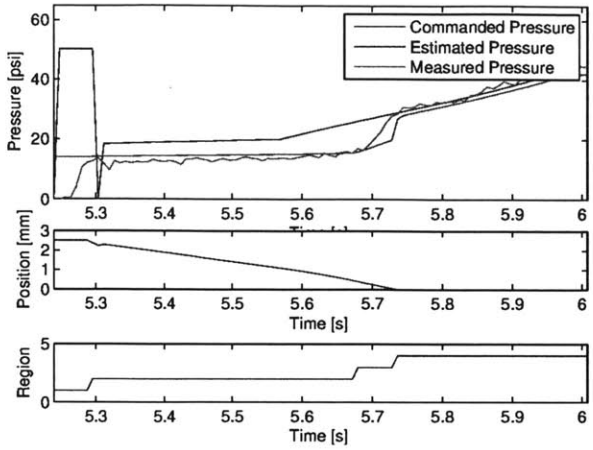

Figure A-12: Example of under-boost from 60% pedal command.

A.3 Over-stroke

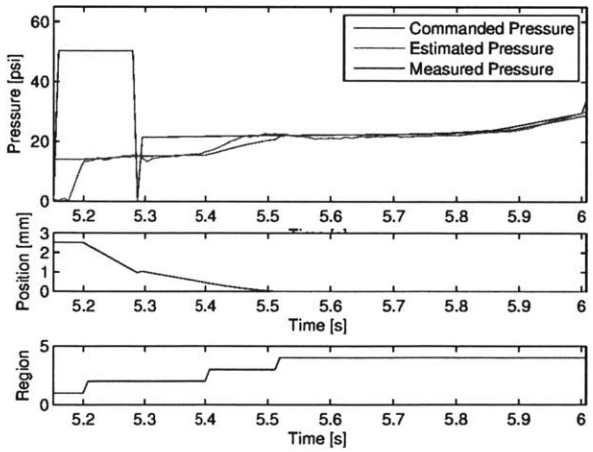

Figure A-13: Example of over-stroke from 10% pedal command.

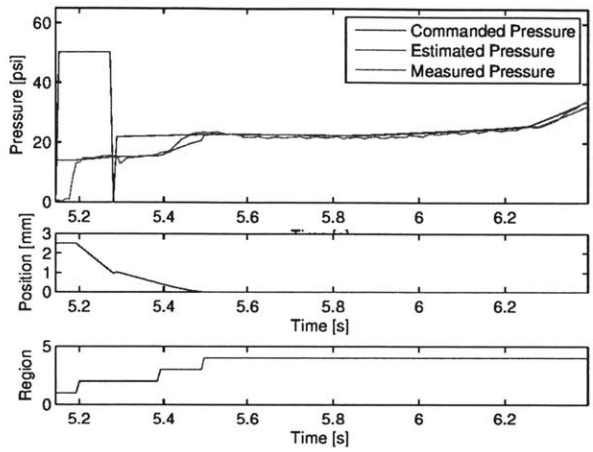

Figure A-14: Example of over-stroke from 15% pedal command.

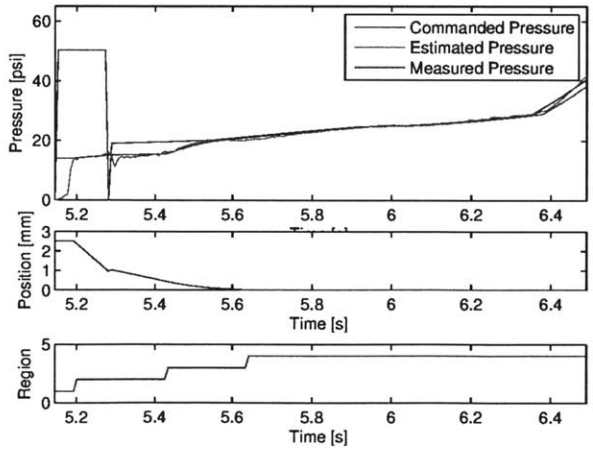

Figure A-15: Example of over-stroke from 20% pedal command.

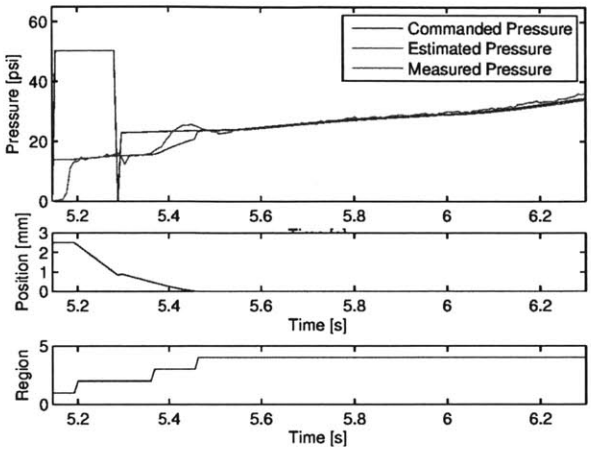

Figure A-16: Example of over-stroke from 25% pedal command.

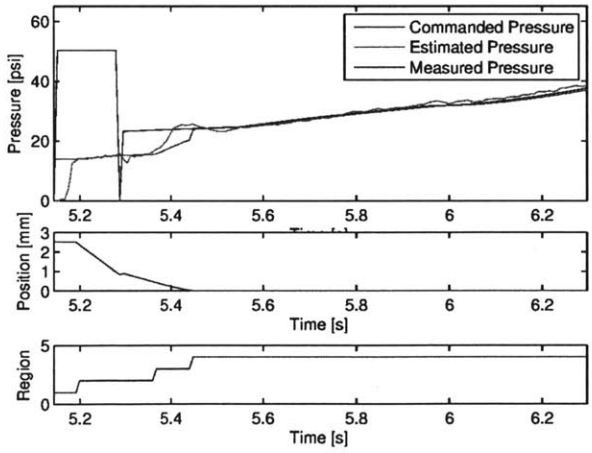

Figure A-17: Example of over-stroke from 30% pedal command.

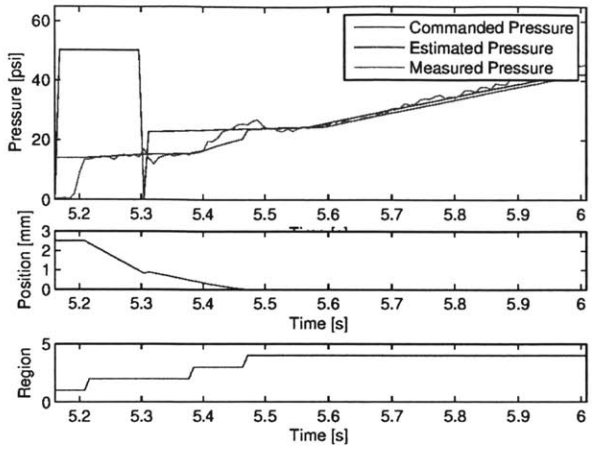

Figure A-18: Example of over-stroke from 60% pedal command.

A.4 Under-stroke

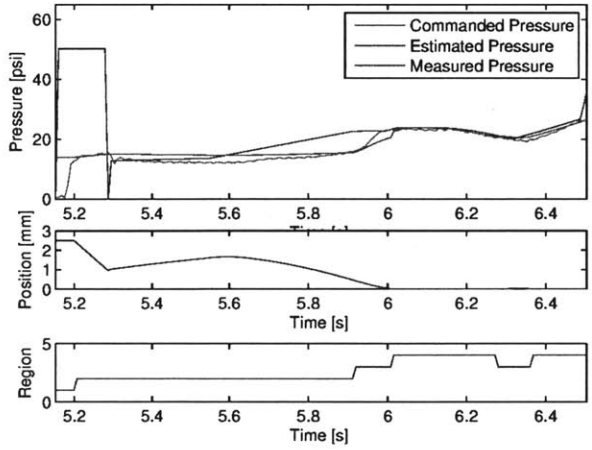

Figure A-19: Example of under-stroke from 10% pedal command.

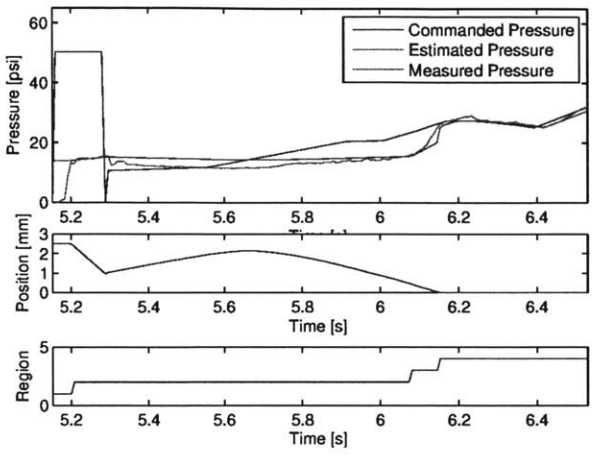

Figure A-20: Example of under-stroke from 15% pedal command.

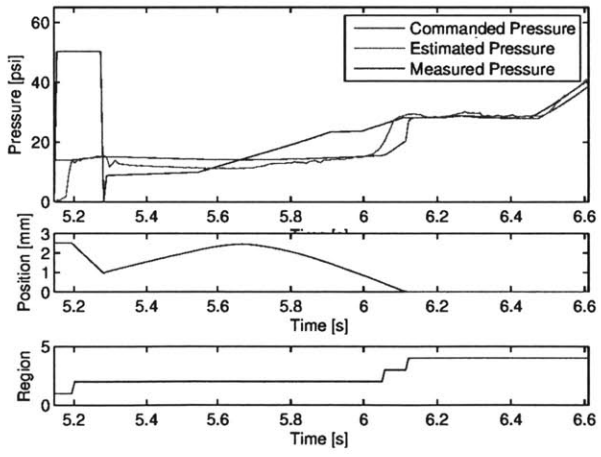

Figure A-21: Example of under-stroke from 20% pedal command.

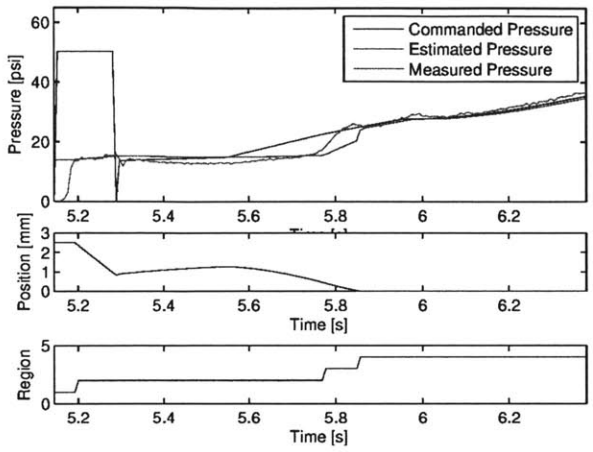

Figure A-22: Example of under-stroke from 25% pedal command.

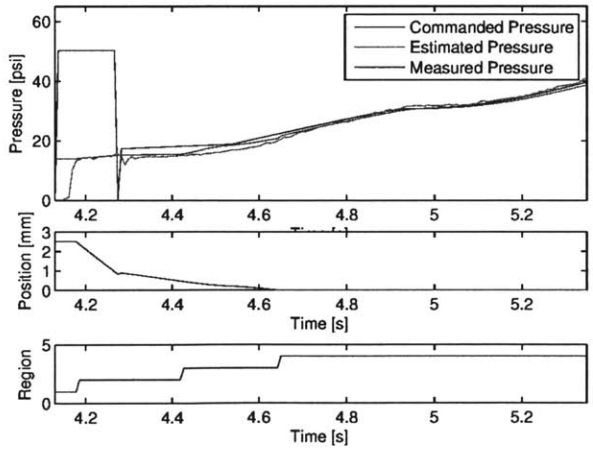

Figure A-23: Example of under-stroke from 30% pedal command.

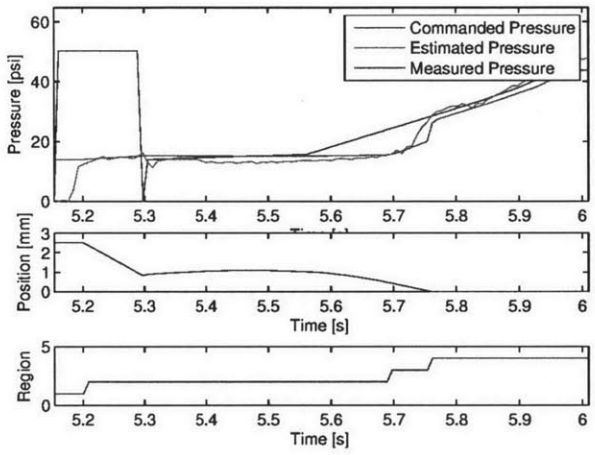

Figure A-24: Example of under-stroke from 60% pedal command.

THIS PAGE INTENTIONALLY LEFT BLANK

Appendix B

Robustness Analysis Results of Off-Nominal Parameter Variations

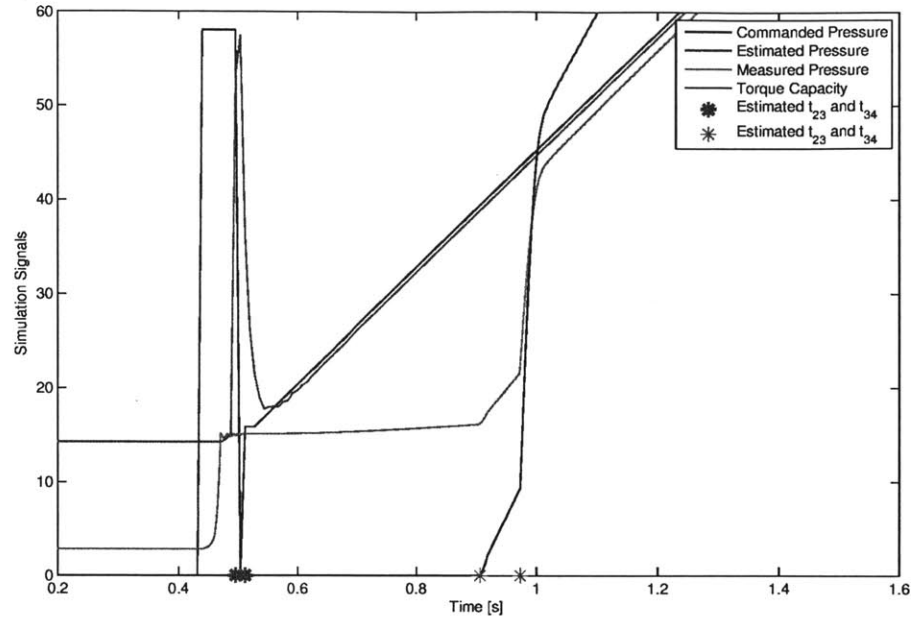

(a)

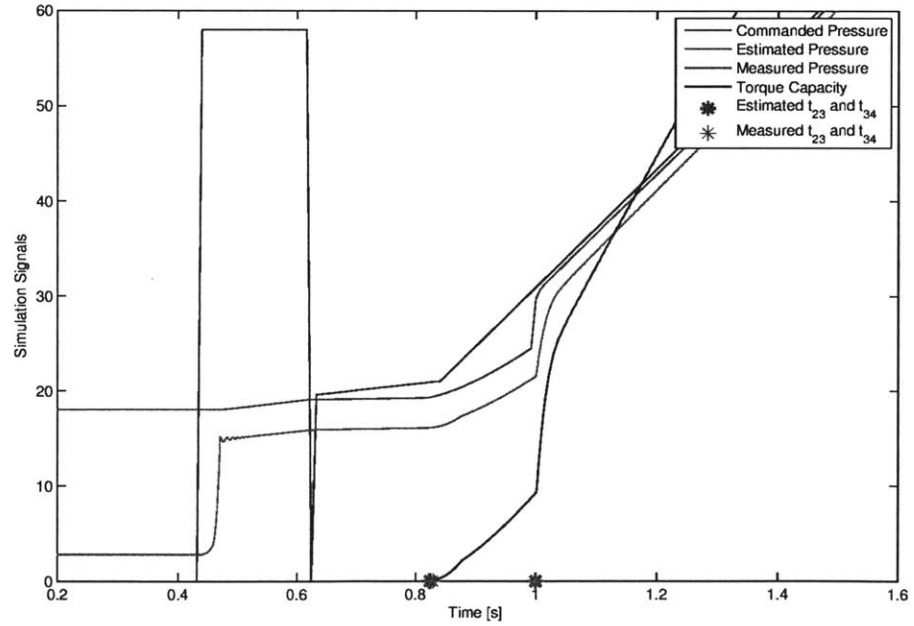

(b)

Figure B-1: Off-nominal condition of -10% x_{max} comparison of (a) first shift using initial condition and (b) final converged shift using adapted values.

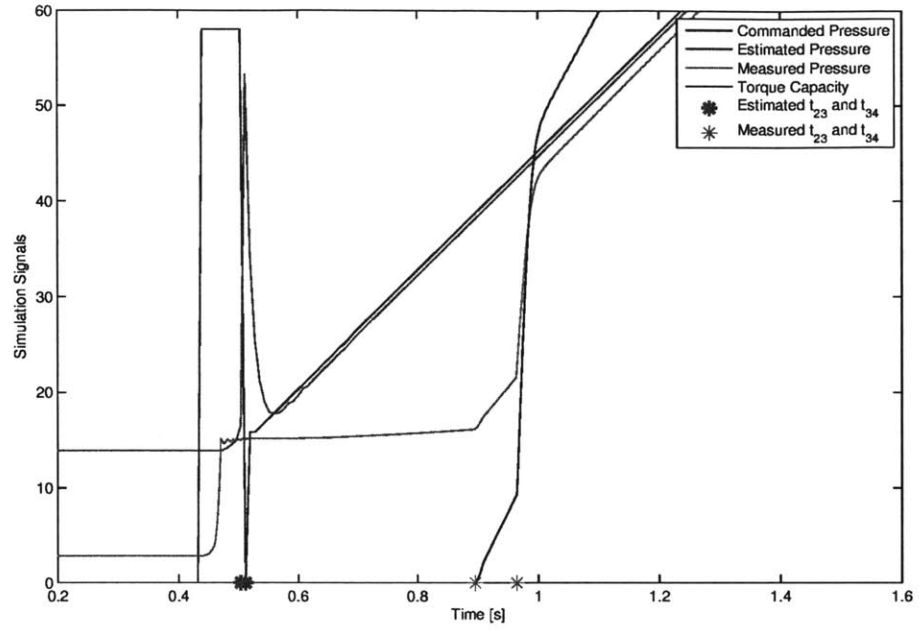

(a)

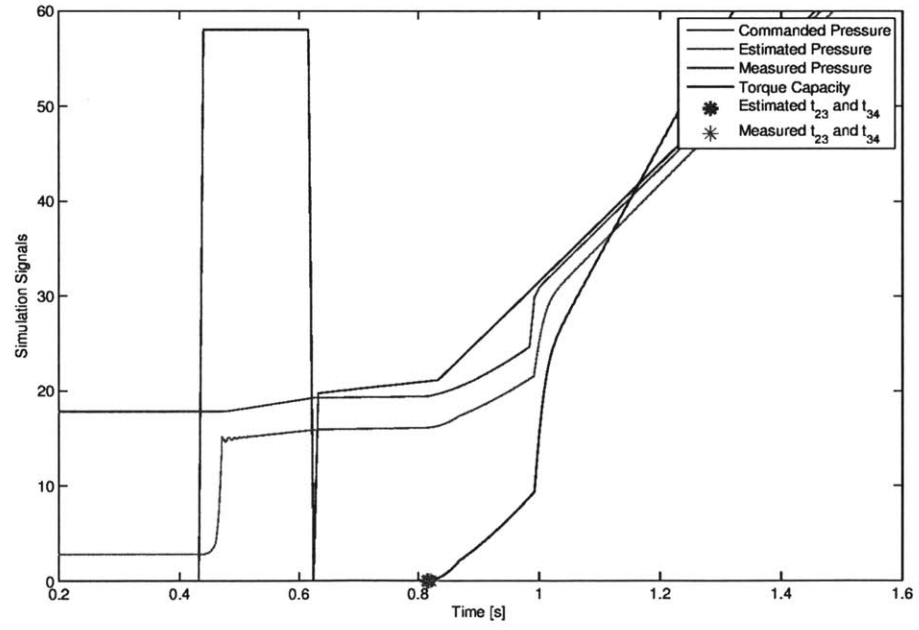

(b)

Figure B-2: Off-nominal condition of +10% x_{max} comparison of (a) first shift using initial condition and (b) final converged shift using adapted values.

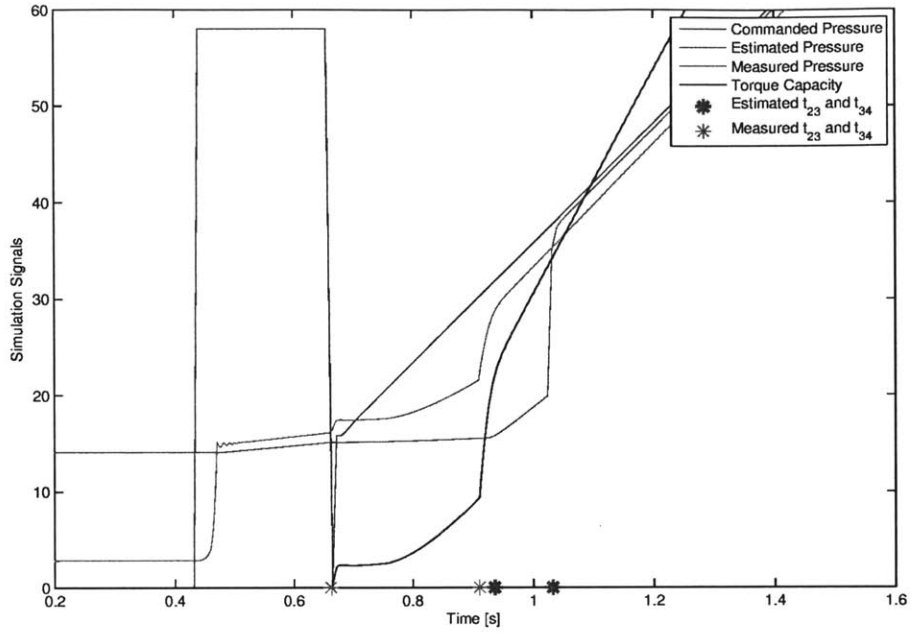

(a)

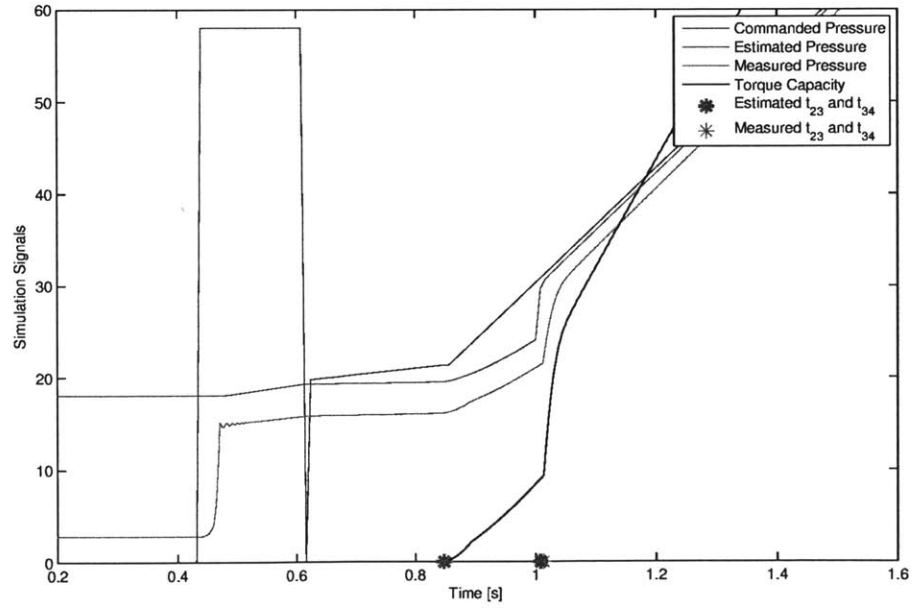

(b)

Figure B-3: Off-nominal condition of -10% x_{free} comparison of (a) first shift using initial condition and (b) final converged shift using adapted values.

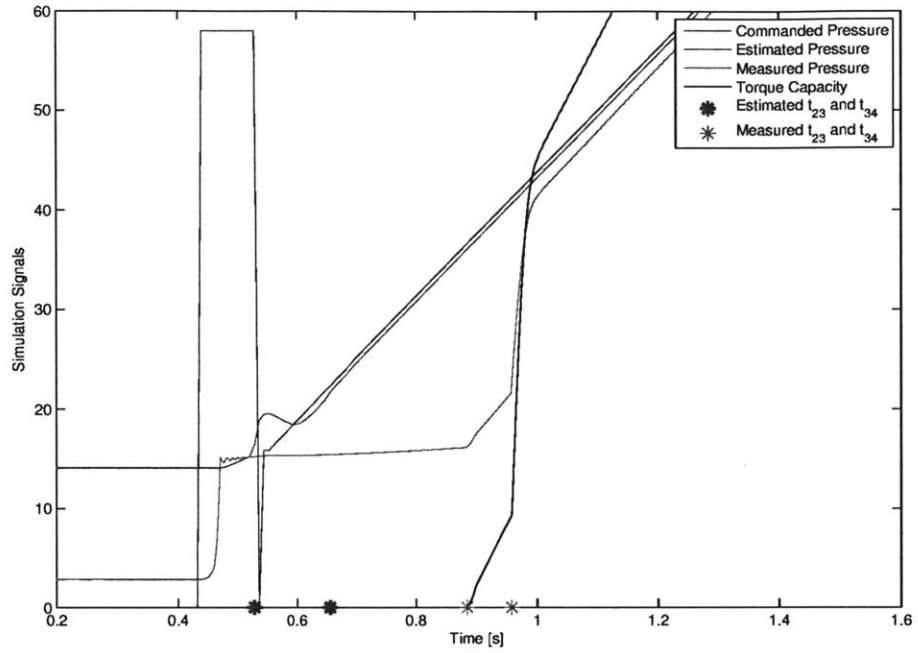

(a)

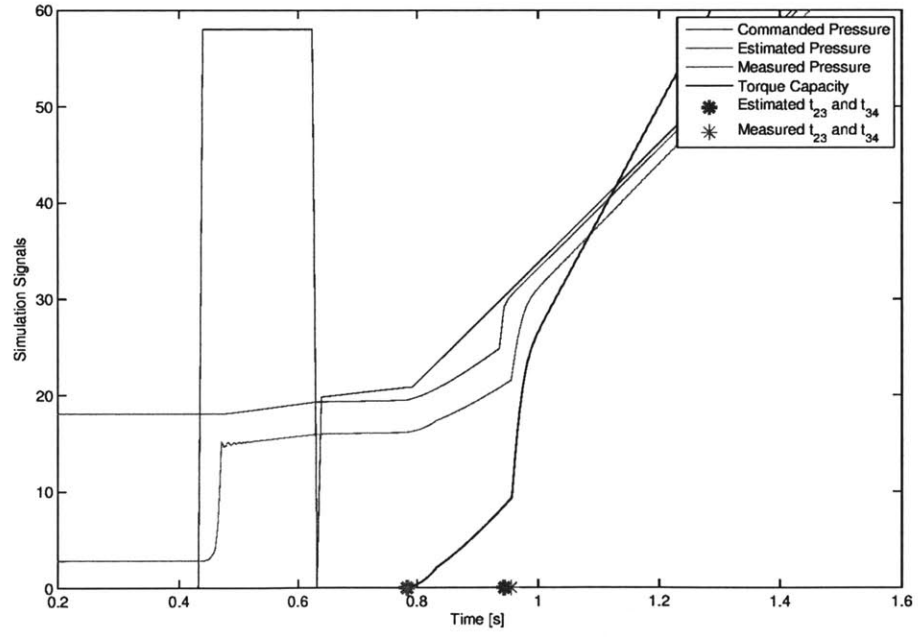

(b)

Figure B-4: Off-nominal condition of +10% x_{free} comparison of (a) first shift using initial condition and (b) final converged shift using adapted values.

THIS PAGE INTENTIONALLY LEFT BLANK

Bibliography

[1] D. Cho and J. K. Hedrick. Automotive powertrain modeling for control. *Journal of Dynamic Systems, Measurement, and Control*, 111(4):568–576, 1989.

[2] B. Depraetere, G. Pinte, and J. Swevers. Iterative optimization of the filling phase of wet clutches. In *Advanced Motion Control, 2010 11th IEEE International Workshop on*, pages 94–99, March 2010.

[3] D. Filev, T. Larsson, and L. Ma. Intelligent control for automotive manufacturing-rule based guided adaptation. In *Industrial Electronics Society, 2000. IECON 2000. 26th Annual Conference of the IEEE*, volume 1, pages 283–288. IEEE, 2000.

[4] D. Filev, L. Ma, and T. Larsson. Adaptive control of nonlinear mimo systems with transport delay: conventional, rule based or neural? In *Fuzzy Systems, 2000. FUZZ IEEE 2000. The Ninth IEEE International Conference on*, volume 2, pages 587–592. IEEE, 2000.

[5] D. P. Filev, S. Bharitkar, and M. F. Tsai. Nonlinear control of static systems with unsupervised learning of the initial conditions. In *Fuzzy Information Processing Society, 1999. NAFIPS. 18th International Conference of the North American*, pages 169–173. IEEE, 1999.

[6] P. E. Gill, W. Murray, and M. H. Wright. *Practical optimization.* Academic press, 1981.

[7] P.E. Gill, W. Murray, M.A. Saunders, and M.H. Wright. Procedures for optimization problems with a mixture of bounds and general linear constraints. *ACM Transactions on Mathematical Software*, 10:282298, 1984.

[8] P.E. Gill, W. Murray, and M.H. Wright. *Numerical Linear Algebra and Optimization*, volume 1. Addison Wesley, 1991.

[9] D. Hrovat, J. Asgari, and M. Fodor. Mechatronic systems techniques and applications. volume 2, chapter Automotive mechatronic systems, pages 1–98. Gordon and Breach Science Publishers, Inc., Newark, NJ, USA, 2000.

[10] D. Hrovat and W. F. Powers. Computer control systems for automotive power trains. *Control Systems Magazine, IEEE*, 8(4):3–10, August 1988.

[11] T. Larsson, L. Ma, and D. Filev. Adaptive control of a static multiple input multiple output system. In *American Control Conference, 2000. Proceedings of the 2000*, volume 4, pages 2573–2577. IEEE, 2000.

[12] L. Ljung. *System Identification.* Wiley Online Library, 1999.

[13] L. S. Louca, J. L. Stein, G. M. Hulbert, and J. Sprague. Proper model generation: An energy-based methodology. *Simulation Series*, 29:44–49, 1997.

[14] R. A. Masmoudi and J. K. Hedrick. Estimation of vehicle shaft torque using nonlinear observers. *Journal of Dynamic Systems, Measurement, and Control*, 114(3):394–400, 1992.

[15] S. Thornton, G. M. Pietron, D. Yanakiev, J. McCallum, and A. Annaswamy. Hydraulic clutch modeling for automotive control. Submitted to 52nd IEEE Conference on Decision and Control, 2013.

[16] Y. Wang, M. Kraska, and W. Ortmann. Dynamic modeling of a variable force solenoid and a clutch for hydraulic control in vehicle transmission system. In *Proceedings of the American Control Conference, 2001*, volume 3, pages 1789–1793, June 2001.

[17] S. Watechagit. *Modeling and Estimation for Stepped Automatic Transmission with Clutch-to-Clutch Shift Technology.* PhD thesis, The Ohio State University, 2004.

[18] D. Yanakiev, Y. Fuji, E. Tseng, G. M. Pietron, and J. F. Kucharski. Closed-loop torque phase control for shifting automatic transmission gear ratios based on friction element load estimation. Ford Global Technologies, December 2010. US Patent Application 20100318269.